OXIDATION RATES AND POLLUTION LOADS IN DRAINAGE; CORRELATION OF MEASUREMENTS IN A PYRITIC WASTE ROCK DUMP[1]

J.W. Bennett,[2] D.K. Gibson,[2] A.I.M. Ritchie,[2] Y. Tan,[2] P.G. Broman,[3] and H. Jönsson[3]

Abstract: There are several methods by which the oxidation rate in a pyritic waste rock dump may be inferred. Pore gas oxygen concentration profiles, temperature profiles, and drainage-monitoring data have been analysed to quantify the oxidation processes occurring in a waste rock dump at the Aitik Mine in northern Sweden. Analysis of oxygen concentration profiles showed that material in some regions of the portion of the dump investigated had an intrinsic oxidation rate (IOR) of about 10^{-8} kg m^{-3} s^{-1} which was some 60 times greater than that of material in other regions. A comparison with pollution loads from measurements in the cutoff drain indicates that if 14% of the dump has an IOR of 10^{-8} kg m^{-3} s^{-1} then 86% has an IOR that contributes little to the total pollution load from the dump. The higher IOR found for the Aitik waste rock dump material is about eight times lower than the highest value found for waste rock at Rum Jungle in northern Australia. It is stressed, however, that the comparatively low IOR of the Aitik waste rock dump material still generates significant pollution loads in drainage. The case study presented emphasizes the utility of using temperature and oxygen profile measurements together with flow and concentration measurements to characterize pollution generation and drainage from a dump.

Additional Key Words: acid mine drainage, oxygen concentration, temperature, gas diffusion, sulfate.

Introduction

The primary process that leads to pollution generation in a pyritic waste rock dump is the oxidation of the pyrite. For this reason it is important to have data on the rate at which this reaction proceeds in a dump. The overall dump oxidation rate, which is the space integral of the oxidation rate over the dump at any one time, is a direct measure of the primary pollution generation rate in the waste rock dump and a major determinant of pollution loads in drainage from the dump. The intrinsic oxidation rate (IOR), for any one particular type of waste rock, is a function that relates the oxidation rate to any parameters that might be considered relevant, such as the oxygen and pyrite concentrations, the dump temperature, local pH, and so forth. An approximation to this function is required in most modeling of dump behavior.

There are several methods by which the oxidation rate in a pyritic waste rock dump may be inferred. One is the analysis of oxygen concentration profiles within the dump. Analysis is straightforward if diffusion is the dominant oxygen transport process. The IOR, in units of kilograms of oxygen consumed per cubic meter of rock per second, is readily inferred from the pore gas oxygen concentration profiles and the diffusion coefficient for oxygen in the waste rock.

Another approach is to measure the temperature rise brought about by the exothermic oxidation process. Interpretation of temperature measurements may be made difficult by the effects of seasonal variations in solar radiation and uncertainties about the boundary conditions at the base of the dump. Despite this, reasonable estimates of oxidation rates have been derived by this means (Harries and Ritchie 1981).

---

[1] Paper presented at the International Land Reclamation and Acid Mine Drainage Conference and the Third International Conference on the Abatement of Acidic Drainage, Pittsburgh, PA, April 24-29, 1994.

[2] John Bennett, Senior Research Scientist, David Gibson, Principal Research Scientist, Ian Ritchie, Senior Principal Research Scientist, and Yunhu Tan, Research Scientist, Australian Nuclear Science and Technology Organisation, Lucas Heights, NSW, Australia.

[3] Per Broman, Vice President Environment, and Hans Jönsson, Project Manager, Boliden Mineral AB, Boliden, Sweden.

The third approach is to measure the rate of output of chemical species in drainage water and infer the oxidation rate in the dump (for example, Galbraith 1991). Sulfate makes a good tracer for the oxidation of pyrite because it is a direct product of the reaction and is abundant, reaching concentrations of a few grams per liter. Care must be taken however to ensure that it is conservative through the system. The average sulfate load, in units of tonnes per year can be measured relatively easily if good measurements of sulfate concentration and flow rate of drainage from the dump are available.

The application of these techniques to a waste rock dump at the Aitik copper mine in northern Sweden is discussed in this paper.

Background and Field Measurements

Aitik Waste Dumps

The Aitik Mine is located near the town of Gällivare in the north of Sweden, about 100 km north of the Arctic Circle. Aitik is operated by Boliden Mineral AB and is Europe's largest copper mine. The opencut operation which was begun around 1960 now produces approximately 14 million tonnes of waste rock per year and about the same quantity of mill tailings. The waste rock from the pit has been disposed of by end-dumping from trucks in dumps which currently average about 25 m in height and cover an area of about 400 ha.

The ore deposit at Aitik consists principally of biotite gneiss, and the waste rock also contains muscovite schist and skarn-banded gneiss. Chalcopyrite and pyrite are the dominant sulfides, with the pyrite content in the waste rock varying from 0 to 5 wt%, and averaging about 1%. The oxidation of pyrite can be taken then as the sole oxygen-consuming reaction in the Aitik dumps.

The average annual temperature at the site is just above 0°C, ranging from an average of 13.2°C in July to -13.5°C in January. The average precipitation is 680 mm/yr and the net infiltration rate into the waste rock dumps is about 500 mm/yr (Axelsson et al. 1992). From the middle of October to the middle of April the precipitation falls as snow, which then melts over a period of about 6 weeks to the end of May.

Site Selection

The waste rock dump at the southwestern corner of the opencut pit was known to be a source of pollution and was chosen for detailed study. This dump was started around 1975 and had been left undisturbed since about 1989. The area met the criteria that the site be accessible to machinery, contain relatively old waste rock material, have had no rehabilitation works, and would be left undisturbed for the 2-yr timescale of the project. A further advantage of the site was that there was a cutoff drain that collected the drainage from the dump and provided an effective means of monitoring pollutant loads and waterflows. The site tailings dam was upstream of this dump.

Temperature and Oxygen Measurements

Probe holes were drilled in the dump in April and August 1991 using rotary percussion airblast, with steel casing and a 140-mm eccentric bit. Once the casing was removed, the holes were lined with PVC plumbing pipe, 50 mm in external diameter, and capped at the bottom to exclude moisture and so prevent any possible perturbation of the temperature profile in the liner by vapor transport.

Nylon pressure tubing, 3/16-in internal diameter, was attached with adhesive glass filament tape to the outside of the PVC pipe. A tube ran the full length of the liner, from the bottom cap to the top of the pipe, and then one tube ran from each successive meter up to the top. These nylon tubes were to enable pore gas samples to be removed from the dump for determination of the oxygen concentration. The top of the tubes were attached to schrader valves and mounted on a brass plate.

The gap between the drilled hole and the inserted liner was backfilled using builders' sand, with the aim of limiting gas transmission between the ports since the gas diffusion coefficient of sand is not less than that of the dump material. A plug of concrete was put in the top 30 cm of the hole to prevent preferential flow of rainwater along the liner. The suitability of this liner design for temperature profile measurements has been established by Harries and Ritchie (1981).

Figure 1 shows the section of the 130 hectare dump under study and indicates the locations of the 11 probe holes. It can be seen that six holes penetrate the base of the dump.

Pore gas oxygen concentrations were determined by passing gas samples across a commercially available oxygen fuel cell. This enabled oxygen concentrations to be measured from 0% to 20.95%, with an accuracy of better than 0.05%. Temperatures were measured at meter intervals with a precision of ±0.02°C using a calibrated thermistor which was lowered down the PVC pipe. Temperature and oxygen profiles were measured at roughly monthly intervals throughout the project.

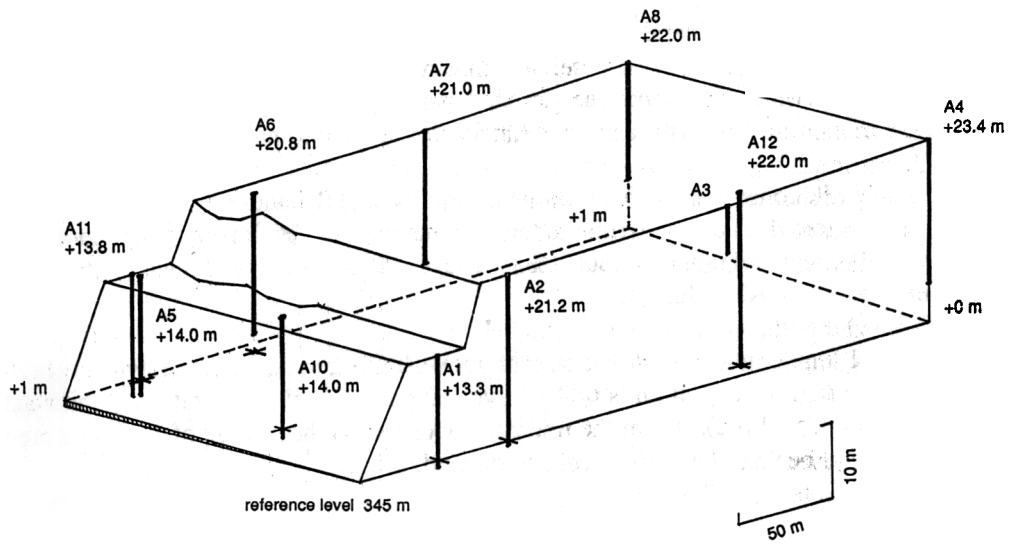

Figure 1. The relative location of the probe holes on the dump used for temperature and oxygen measurements.

Drain and Weir Measurements

To deduce the overall oxidation rate in any given waste rock dump from drainage measurements, it is necessary to know the total load of a relevant pollutant from the dump. This can be obtained by measuring the total water flow through the dump and the concentration of pollutant in the drainage water. Care must be taken that losses of infiltrating water, e.g., to deep ground water, are small. One must also know that the drainage does not contain pollutants from another source. In practice, if either of these complications arise, it may be accounted for if the extent of the loss or gain of pollutant can be estimated. As the flows, concentrations, and loads may vary greatly owing to seasonal factors, regular measurements must be taken at least over a 12-month period.

The glacial till below the Aitik dumps has such a low hydraulic conductivity (Axelsson et al. 1992) that essentially all the water infiltrating them appears at the toe of the dumps and may be collected in cutoff drains. All the flow from the 130 ha dump under study was collected in one drain which had been installed with several flow weirs. Flow rates were measured at various times, the frequency of measurement depending on the season; when flow rates changed quickly during the spring snowmelt measurements were made every few days. Water samples were taken at the time of flow determination and sent to a laboratory for chemical analysis.

Sulfate concentrations were measured to determine the dump oxidation rate for the reasons given above. This

approach requires the sulphate to be conserved in the system. The most common reason for the removal of sulphate from solution flow in dumps is the precipitation of gypsum when the calcium concentration is above the gypsum solubility limit. Ion analysis of the Aitik drainage waters showed the calcium concentrations to be well below this limit.

Analysis of Oxygen Profiles

The rate of pollutant production from the oxidation of pyrite in a waste rock dump can be deduced from estimates of the rate of oxygen consumption in the dump, which in turn is derived from an analysis of measured pore gas oxygen concentration profiles.

Where oxygen diffusion is the sole supply mechanism, oxygen is transported from regions of higher pore gas oxygen concentration to regions of lower concentration. A section of measured profile with constant gradient indicates that oxygen is being transmitted without consumption, whereas a curved profile denotes a region where oxygen is being consumed.

Oxygen profiles can be interpreted qualitatively to infer the dominant gas transport mechanism in a dump and the relative magnitude of pyritic oxidation rates in different regions. Vertical profiles in which the oxygen concentration decreases monotonically with depth are consistent with oxygen being supplied from the top surface by diffusion, higher gradients implying higher oxygen consumption rates in the dump. This is discussed more completely below. Zones of relatively higher oxygen concentrations at depth suggest that either advective transport processes are dominant or there is significant diffusion from the sides. Advection will be accompanied by elevated temperatures resulting from the heat generated by higher oxidation rates.

If it can be assumed that the gas diffusion coefficient does not vary greatly with location, as is most usually the case in waste rock dumps, then it follows that different gradients in the oxygen concentration profiles are due to different oxidation rates.

In the absence of advection (including convection), one-dimensional oxygen transport into the dump by diffusion from the surface can be described as

$$\varepsilon_g \frac{\partial C}{\partial t} = D\frac{\partial^2 C}{\partial x^2} - S(x, t) \tag{1}$$

where C is the pore gas oxygen concentration, t is time, x is distance, D is the oxygen diffusion coefficient, ε_g is the gas-filled pore space, and S is the volume oxygen absorption rate.

The analytical approach requires a knowledge of the diffusion coefficient of the dump material but this does not present such a big problem as it might seem. The primary requirement in characterizing an oxidising dump is to establish oxidation rates to within an order of magnitude so a variation in D by some factors is of little consequence. In practice, the values of D fall within a narrow range because the diffusion coefficient is largely governed by a fixed parameter, the coefficient for diffusion of oxygen in air (under the narrow range of temperature and pressure encountered), and one that has a narrow range of variation, the gas-filled porosity of the dump. The gas diffusion coefficient is not expected to show much spatial variation in any given dump either because of the relative uniformity of porosity and moisture content found in typical waste rock dumps.

In most waste rock dumps the timescale for oxidation of pyrite is much longer than the timescales for gas transport. The oxygen profiles are then pseudo steady state and equation 1 can be simplified to

$$D\frac{\partial^2 C}{\partial x^2} - S(x) = 0. \tag{2}$$

So, if an analytic function can be found to represent a particular oxygen concentration profile well, and the assumptions on which equation 2 is based are satisfied, then the volume oxygen absorption rates or oxidation rates (S) can be easily found by calculating the second derivative or curvature of the function at a given depth.

Results

Oxygen Results

Typical results from the pore gas oxygen concentration measurement program are presented in figures 2 and 3. In general, the oxygen concentration fell monotonically from the surface of the dump, indicating that the oxygen supply mechanism to the sites of pyritic oxidation was dominated by diffusion.

The measured profiles fell into two groups. There was a region near the edge of the dump (probe holes A1, A2, A5, A10, and A11; see figure 2 for example) where there were high gradients in the oxygen concentration profiles and in the central part of the dump the gradients were low (A3, A4, A6, A7, A8, and A12; see figure 3 for example). In the absence of any significant heating in the dump (see below) and making the assumption that the diffusion coefficient of the waste rock does not vary greatly with location, then it is reasonable to conclude that pyritic oxidation rates are relatively high in the region where the gradients are high, and are relatively low where the gradients are low.

The oxygen profiles in the material oxidizing at the higher rate indicate that oxygen was supplied by diffusion and that the rate was not limited by the oxygen supply rate. This means then that the rate is not dependent on the geometry of the dump or the location of the material in the dump, but is a property of the material itself. Clearly, such material may occur anywhere in the dump.

The oxygen profiles in the region with low oxidation rate settled down in a few weeks after installation of the holes. In the regions of high oxidation rate, however, the profiles were variable with time, as shown in figure 2. Whilst the changes were significant with respect to the accuracy with which the oxygen concentrations were measured, they were still relatively small. As a consequence, it was possible to use the region with the greatest gradient to establish a reasonable upper bound on the oxidation rate within the dump.

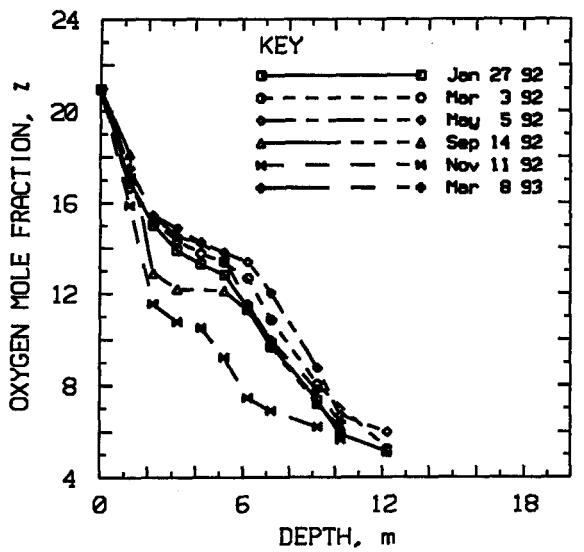

Figure 2. Pore gas oxygen concentrations measured in probe hole A1.

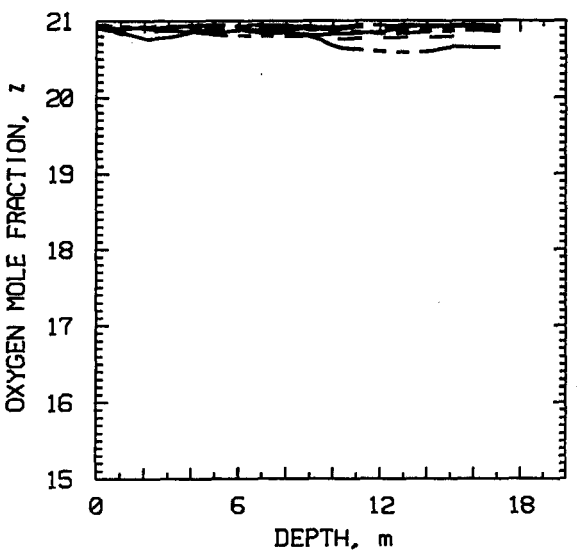

Figure 3. Oxygen concentrations measured in probe hole A7 between April 1991 and January 1992.

So, if an analytic function can be found to represent a particular oxygen concentration profile well, and the assumptions on which equation 2 is based are satisfied, then the volume oxygen absorption rates or oxidation rates (S) can be easily found by calculating the second derivative or curvature of the function at a given depth.

Results

Oxygen Results

Typical results from the pore gas oxygen concentration measurement program are presented in figures 2 and 3. In general, the oxygen concentration fell monotonically from the surface of the dump, indicating that the oxygen supply mechanism to the sites of pyritic oxidation was dominated by diffusion.

The measured profiles fell into two groups. There was a region near the edge of the dump (probe holes A1, A2, A5, A10, and A11; see figure 2 for example) where there were high gradients in the oxygen concentration profiles and in the central part of the dump the gradients were low (A3, A4, A6, A7, A8, and A12; see figure 3 for example). In the absence of any significant heating in the dump (see below) and making the assumption that the diffusion coefficient of the waste rock does not vary greatly with location, then it is reasonable to conclude that pyritic oxidation rates are relatively high in the region where the gradients are high, and are relatively low where the gradients are low.

The oxygen profiles in the material oxidizing at the higher rate indicate that oxygen was supplied by diffusion and that the rate was not limited by the oxygen supply rate. This means then that the rate is not dependent on the geometry of the dump or the location of the material in the dump, but is a property of the material itself. Clearly, such material may occur anywhere in the dump.

The oxygen profiles in the region with low oxidation rate settled down in a few weeks after installation of the holes. In the regions of high oxidation rate, however, the profiles were variable with time, as shown in figure 2. Whilst the changes were significant with respect to the accuracy with which the oxygen concentrations were measured, they were still relatively small. As a consequence, it was possible to use the region with the greatest gradient to establish a reasonable upper bound on the oxidation rate within the dump.

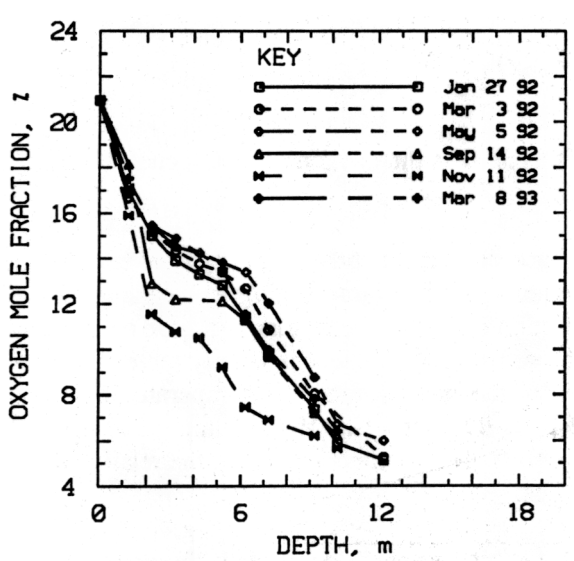

Figure 2. Pore gas oxygen concentrations measured in probe hole A1.

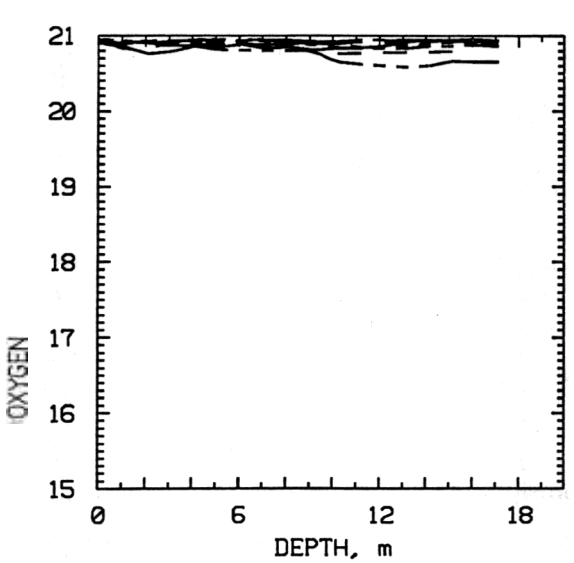

Figure 3. Oxygen concentrations measured in probe hole A7 between April 1991 and January 1992.

Following the method described above, functions of a suitable form were constructed and fitted using a least-squares method to the data points of the oxygen profiles measured in hole A1 over a 2-yr period, from April 1991 to April 1993. Since the oxygen concentration (mole fraction) at the surface of the dump is fixed at 20.95% (atmospheric), the fitted curves were constrained to pass through this point.

Figure 4 presents an example of the graphical results of the best fit of the predetermined function to data measured in the top 6.2 m of hole A1 in May 1992. (The measured profile indicates no oxygen consumption in the waste rock below this depth.) In the figure the axes have been normalized so that the atmospheric oxygen concentration (20.95%) = 1 and the depth of 11.22 m = 1. The normalized data and error estimates are also shown. The function clearly describes the measured pore gas oxygen concentration profiles very well. The second derivative or curvature of the fitted curve at a chosen depth was determined and converted to the volume absorption rate or oxidation rate. The oxygen diffusion coefficient in the dump, D, was taken as 4.1×10^{-6} m^2 s^{-1}, taking the gas-filled porosity as 0.28 and using the curve of Papendick and Runkles (1965). This procedure produced a set of oxidation rates at a series of depths and time.

The oxidation rates thus determined from the hole A1 profiles ranged from $(3.1 \pm 0.2) \times 10^{-9}$ kg m^{-3} s^{-1} to $(4.3 \pm 0.3) \times 10^{-8}$ kg m^{-3} s^{-1}, with an average volume absorption rate for the high oxidation region of the dump of close to 1×10^{-8} kg m^{-3} s^{-1}.

Another method for quantifying oxidation rates in the dump from the measured pore gas oxygen concentration profiles involved obtaining the oxygen fluxes into the top surface of the dump. The gradient of the pore gas oxygen concentration at the surface for each measured profile was determined graphically, and the surface oxygen fluxes were estimated using the oxygen diffusion coefficient given above. The surface oxygen fluxes varied with location, with two distinct classes of surface oxygen fluxes being seen in the test area. In keeping with the earlier analysis, higher fluxes were found at the edge of the dump, with lower fluxes in the central region. The average values of surface oxygen flux into the dump were found to be $(15 \pm 9) \times 10^{-8}$ kg m^{-2} s^{-1} at A1, A2, A5, A10, and A11 and $(0.25 \pm 0.25) \times 10^{-8}$ kg m^{-2} s^{-1} at A3, A4, A6, A7, A8, and A12. The standard deviation on the averages represents flux variations with location and time, although a clear seasonal pattern was not seen.

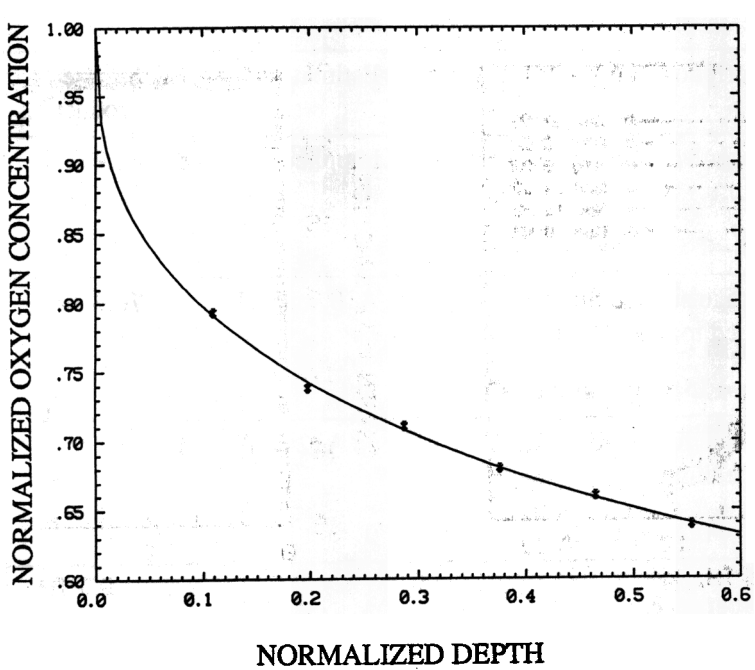

Figure 4. Function fitted to the pore gas oxygen concentration data measured in probe hole A1 in May 1992.

The shape of the oxygen profiles at the bottom of A1 implies a flux through the base of the dump. The average value of this flux was estimated to be 2×10^{-8} kg m^{-2} s^{-1}. The net oxygen flux (oxygen consumed in the dump) is then simply the difference between the surface and bottom oxygen fluxes, which was found to be 13×10^{-8} kg m^{-2} s^{-1}. The flux through the base of the dump in the central region of the dump was taken to be negligibly small, because the gradients at the bottom of the profiles show no indication of such a flux, and because neglecting any flux through the base leads to an overestimate rather than an underestimate of pollution generation in the dump.

The total amount of oxygen consumed in the whole dump can be estimated by using either the surface flux values or the volume oxygen absorption rates. Assuming that all the oxygen diffusing into the dump surface was consumed by pyritic oxidation, then oxygen consumption can be converted into sulfate production using the overall stoichiometry of the reaction of oxygen with pyrite (1 kg oxygen → 1.714 kg sulfate).

Three estimates of the pollution generation rate from the 130 ha dump which drains into the cutoff drain have been made, which effectively put upper and lower bounds on the rate:

1. The average volume absorption rate of 1×10^{-8} kg m^{-3} s^{-1} obtained from hole A1 was applied to the whole dump. At this rate of absorption, diffusion will limit oxidation to the top 15 m of the dump, so the effective thickness of the 130-ha dump is taken to be 15 m. This gives an annual sulfate production rate of 10,500 t/yr.

2. An estimate of 10,000 t/yr of sulfate was obtained by applying the average surface flux at A1, A2, A5, A10, and A11 (15×10^{-8} kg m^{-2} s^{-1}) to the whole dump.

3. A lower bound was estimated by using the average of the six lowest oxygen fluxes (A3, A4, A6, A7, A8, and A12). The average of these fluxes, 0.25×10^{-8} kg m^{-2} s^{-1}, was applied to the whole dump and yielded a rate of 180 t/yr of sulfate.

The results are summarized in table 1, expressed in units of tonnes per hectare per year.

Table 1. Annual Sulfate Production from the 130-ha Dump (t ha^{-1} yr^{-1}).

Description of Method Used for the Estimate	Sulfate production
Oxygen volume absorption rate at A1 applied to whole dump. Rate = 1×10^{-8} kg m^{-3} s^{-1}	80.9
Average surface flux at A1, A2, A5, A10, and A11 applied to whole dump. Flux = 15×10^{-8} kg m^{-2} s^{-1}	76.9
Average flux at A3, A4,A6,A7,A8, and A12 applied to whole dump. Flux = 0.25×10^{-8} kg m^{-2} s^{-1}	1.4

Oxidation Rates From Temperature

Whilst oxidation rates can in principle be obtained from measured temperature profiles, where heat is generated by the pyritic oxidation reaction, this has been found to be too difficult with the Aitik data owing to a number of factors as outlined below.

The ambient average monthly temperatures at the Aitik site range from -13.5°C in January to 13.2°C in July. The near-surface temperatures in the dump follow the ambient ones closely when they are positive, but once the surface freezes the dump temperatures do not drop below -5°C. During the months when the dump surface is warming up, the temperature in the dump is highest at the surface, but as the surface cools down, the temperature peak travels deeper into the dump. The attenuation and phase shift of the Fourier components of the temperature signal at the surface depend on the thermal properties of the dump.

Figure 5 shows the temperature profiles measured in hole A1 over a 10-month period and illustrates how the large seasonal swing in surface temperatures affects the temperature of the dump to a depth of at least 10 m. Because the average ambient temperature at the site is close to 0°C, the temperature of about 2.5°C which is seen in the lower part of the dump can be attributed to heating due to pyritic oxidation. This is a relatively small signal, especially when compared with the temperature fluctuations due to insolation in the top half of hole A1, where the oxidation has been found to be occurring.

A further difficulty with any analysis of the temperature data is that the boundary condition at the base of the dump is unknown. Water is flowing close to the interface between the dump and the original ground surface and will have affect measured temperature distributions, but not enough is known about the system to be able to quantify this reliably.

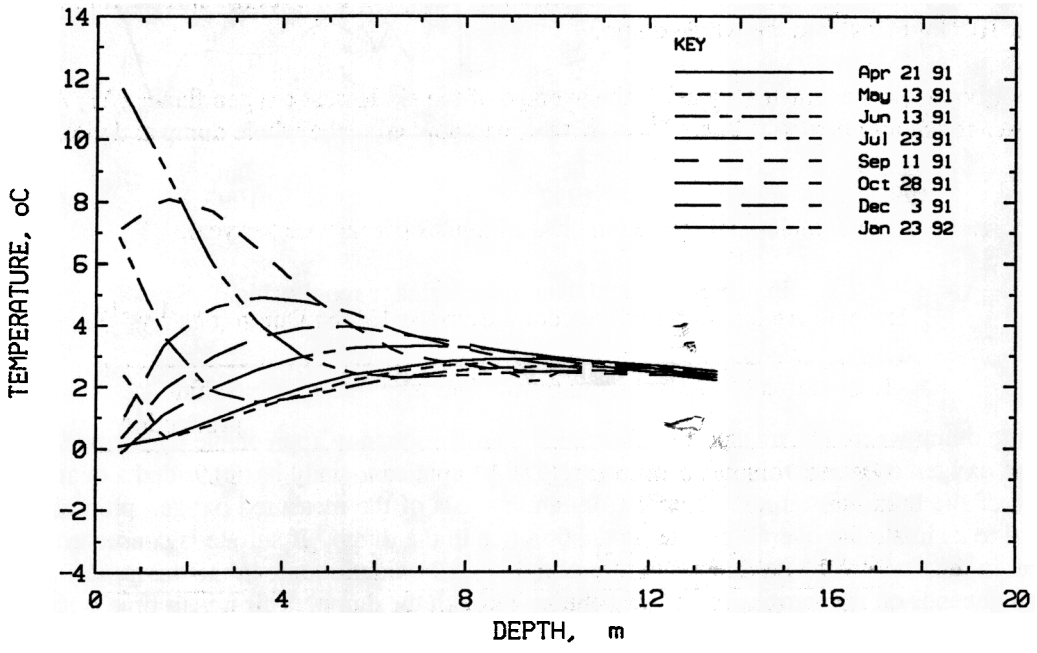

Figure 5. Temperature profiles measured in probe hole A1.

Flows, Concentrations and Loads

Figure 6 shows a typical result for the monitoring in the cutoff drain of drainage flow rates and sulfate concentrations. The instantaneous load is the product of the flow and concentration. The average annual load was obtained by integrating the load over the period. A careful analysis of the water balance and drainage data showed that a constant sulfate load was coming from the tailings dam, underflowing the waste rock dump and entering the cutoff drain. This load was subtracted from the total load in the drain to give a value of 12.1 t ha^{-1} yr^{-1} for the annual sulfate

production of the waste rock dump. As presented in table 1, the annual sulphate production rate from the high and low IOR material in the dump has been estimated to be 80.9 t ha^{-1} yr^{-1} and 1.4 t ha^{-1} yr^{-1}, respectively. The drain data implies, then, that 14% of the dump is composed of the high IOR material and the rest has the low IOR.

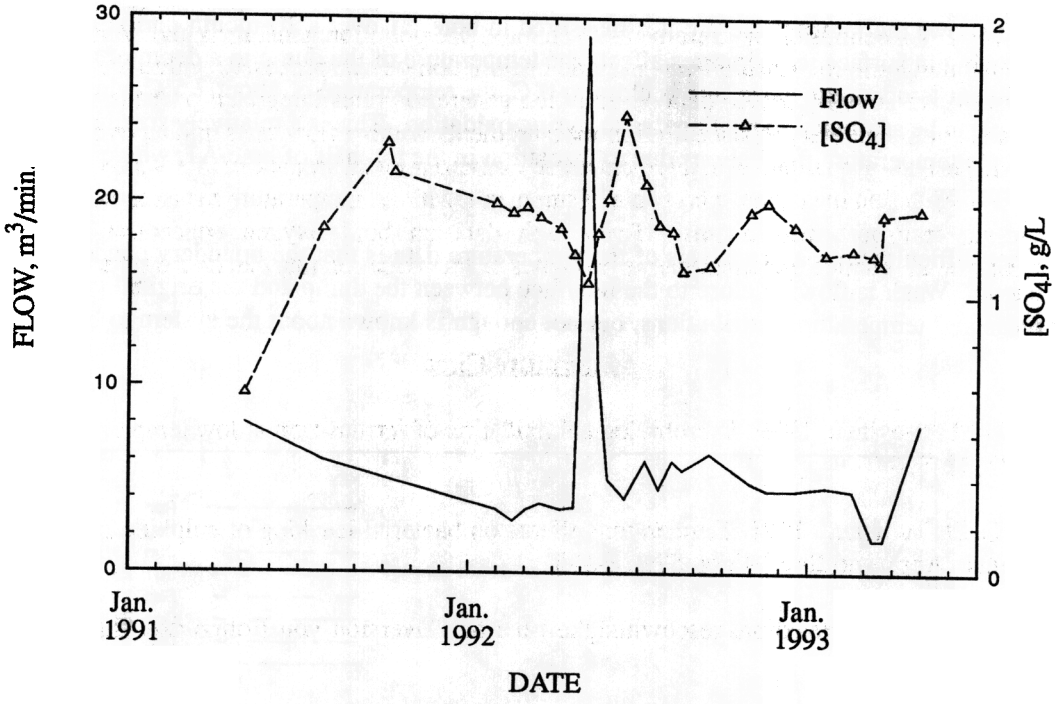

Figure 6. Typical data from drainage monitoring.

Discussion and Conclusions

In a large dump where gas transport is dominated by diffusion, any appreciable pyrite oxidation rate leads to a reduction in the oxygen concentration in the pore gas. The present case study has provided a quantitative estimate of oxidation rates of the bulk waste rock material from an analysis of the measured oxygen profiles. These oxidation rates were used to estimate the overall sulfate production rate in the dump. If sulfate is conserved in the system then the sulfate load in the drain will be a direct measure of the overall oxidation rate in the dump, shifted in time by some function which depends on the transit time of the solution through the dump. This transit time is short, of the order of a few years in typical dumps, compared with the time to oxidize the whole dump.

Analysis of oxygen concentration profiles showed that material in some regions of the dump investigated had an IOR of about 10^{-8} kg m^{-3} s^{-1} which was some 60 times greater than that of material in other regions. A comparison with pollution loads from measurements in the cutoff drain indicates that if 14% of the dump has an IOR of 10^{-8} kg m^{-3} s^{-1} then 86% has an IOR that contributes little to the total pollution load from the dump.

The temperature rise in the dump from heat produced in the pyritic oxidation reaction was too small to extract the oxidation rate from the temperature profiles, particularly in the top 6 m of the dump, where the changes caused by seasonal temperature changes were large. Hence, although in principle the oxidation rate can be extracted from both the temperature and oxygen concentration profiles in the dump, in practice it was possible to use only one of these methods.

It is important to note that the "high" IOR found for the Aitik waste rock dump material is about eight times lower than the highest value found for waste rock at Rum Jungle in northern Australia (Harries and Ritchie 1981). It should be stressed, however, that a comparatively low IOR such as that found for the Aitik waste rock dump material still generates significant pollution loads in drainage. The main reason is that in the early history of the dump, which may last for many years, a low IOR means that a large region of dump is involved in oxidation.

The case study presented here has emphasized the utility of using pore gas oxygen profile measurements together with flow and concentration measurements to characterize pollution generation and drainage from a dump. In general, oxygen and temperature measurements provide information on rate processes within the dump, while the flow and concentration measurements provide data on pollution generation rates integrated over the whole dump. The set of measurements is complementary. Concentration measurements without flow rates and an overall water balance for the dump lead, at best, to a qualitative assessment of the environmental impact of the waste rock dump or of the effectiveness of rehabilitation measures. Oxygen measurements without temperature measurements can lead to wrong conclusions on gas transport mechanisms. Even with data on both oxygen concentrations and temperature distributions it may be in practice that quantitative estimates of the oxidation rate can be extracted from only one set of data.

Literature Cited

Ahonen, L. and O. H. Tuovinen. 1989. Microbiological oxidation of ferrous iron at low temperatures. Appl. and Env. Micro. 55:312-316.

Ahonen, L. and O. H. Tuovinen. 1991. Temperature effects on bacterial leaching of sulphide minerals in shake flask experiments. Appl. and Env. Micro. 57:138-145.

Arrhenius, S. 1889. Uber die Reaktionsgeschwindigkeit bei der Inversion von Rohrzucker durch Sauren. Z. Phys. Chem. 4:226-248.

Axelsson, C.L., J. Byström, J. Holmén, and T. Jansson. 1992. Efterbehandling av sandmagasin och gråbergsupplag i Aitik, Hydrogeologiska förutsättningar för åtgärdsplan. Report 927-1801 (in Swedish), Golder Geosystem AB.

Ferroni, G. D., L. G. Leduc, and M. Toddm. 1986. Isolation and temperature characterization of psychrotrophic strains of *Thiobacillus ferrooxidans* from the environment of a uranium mine. J. Gen. Appl. Micro. 32:169-175.

Galbraith, D.M. 1991. The Mount Washington acid mine drainage reclamation project. p. 145-161. In Proceedings of Second International Conference on the Abatement of Acidic Drainage, v. 2. (Montreal, PQ, September 16-18, 1991).

Harries, J.R. and A.I.M. Ritchie. 1981. The use of temperature profiles to estimate the pyritic oxidation rate in a waste rock dump from an open-cut mine. Water, Air, Soil Pollution 15:405-423.

Okerke, A, and S. E. Stevens. 1991. Kinetics of iron oxidation by *Thiobacillus ferrooxidans*. Appl. and Env. Micro. 57:1052-1056.

Papendick, R. I. and J. R. Runkles. 1965. Transient-state oxygen diffusion in soil: I. The case when rate of oxygen consumption is constant. Soil Science 100(4):251-261.

MONITORING GASEOUS AND LIQUID FLUX IN SULFIDE WASTE ROCK[1]

William M. Schafer[2], Steven Smith[2], Chris Luckay[2] and Troy Smith[3]

ABSTRACT: A monitoring program was used to compare water migration, oxygen concentration, temperature, and solution chemistry in paired reclaimed and unreclaimed sulfide waste rock dumps in southwestern Montana. Slope regrading to a 2:1 gradient, addition of cover-soil, and revegetation appear to limit infiltration. In most locations, pyrite oxidation is only present in the upper 30 ft of the dump the region most affected by the wetting front to date. Waste rock in the lower 100 ft of the dump may be too dry to support microbial oxidation of pyrite.

Additional Key Words: acid mine drainage, hard-rock mining, waste rock, acid drainage abatement, environmental monitoring.

Introduction

Acid mine drainage (AMD) from waste rock disposal facilities is a prevalent concern at a number of Western U.S. hard rock mining sites. Relationships between waste rock geochemistry, internal water movement, and oxygen supply and their effect on surface and groundwater quality and on overall reclamation success are concerns of regulatory agencies. The dynamics of the sulfide oxidation reaction are closely related to waste rock mineralogy and hydrology. Infiltrating water may promote the migration of acidic and metal enriched pore water. While gaseous oxygen is usually abundant within a dump owing to the abundant porosity, heat produced during microbial pyrite oxidation may create a thermally driven advective circuit, in effect pumping oxygen to the reactive core of unreclaimed waste rock dumps (Harries and Ritchie 1987)(Fig. 1).

A number of facility engineering and reclamation practices may be used to minimize the risk of AMD for mine waste facilities in semi-arid areas (Schafer 1992). Regrading of the angle-of-repose dump slope may seal off the permeable "rubble zone" that forms at the base of end-dumped waste. In so doing, the advective oxygen supply may be limited. More importantly, placement of cover-soil and establishment of vegetation may promote surface runoff and increase evaporative consumption of water. In this way off-site AMD can be alleviated by reducing the rate of seepage through the facility. Other engineering practices such as dump construction in thin compacted lifts, and construction of waste cells within clay layers (Krauss 1990) have also been used.

The Golden Sunlight Mine is a large scale open-pit gold producer located in southwestern Montana. Gold is hosted in a breccia pipe system which is superimposed in a thick argillite sequence and quartz latite intrusives. Unoxidized waste rock typically contains 2% to 5% pyritic S and has negligible neutralization capacity. Over 100 million mt of waste rock have been placed in single stage dumps around the perimeter of the pit. Owing to the steep terrain, dump height exceeds 600 ft in some locations.

Reclamation techniques utilized at the Golden Sunlight Mine (Fig. 2) are designed to limit acid production and migration by (1) reducing infiltration of water and (2) reducing the supply of oxygen. Regrading of slopes from all angle of repose of 1.4:1 to 2:1 is designed both to reduce the slope steepness and to seal off rubble zones at the original dump toe, thus reducing the potential for advective air movement into the dump. Application of rock

---

[1]Paper presented at the International Land Reclamation and Mine Drainage Conference and the Third International Conference on the Abatement of Acidic Drainage, Pittsburgh, PA, April 24-29, 1994.

[2]William M. Schafer, Principal, Steven Smith, Senior Scientist, and Chris Luckay, Staff Engineer, Schafer and Associates, Bozeman, MT, USA.

[3]Troy Smith, Reclamation Scientist, Golden Sunlight Mine, Whitehall, MT, USA.

capping material and cover-soil limits water infiltration, increases runoff, and further reduces oxygen movement into the dump. As vegetation becomes established in the applied cover-soil, plant water use and evaporative water loss will increase. Information acquired in this study will enable the long-term effectiveness of waste rock reclamation to be evaluated at the Golden Sunlight Mine.

The objective of this on going investigation is to concurrently monitor the hydrologic conditions in a large unreclaimed angle-of-repose waste rock dump and a paired reclaimed dump. A combination of downhole monitoring techniques was used to measure differences in gaseous oxygen concentrations, temperature, water content, and pore water chemistry.

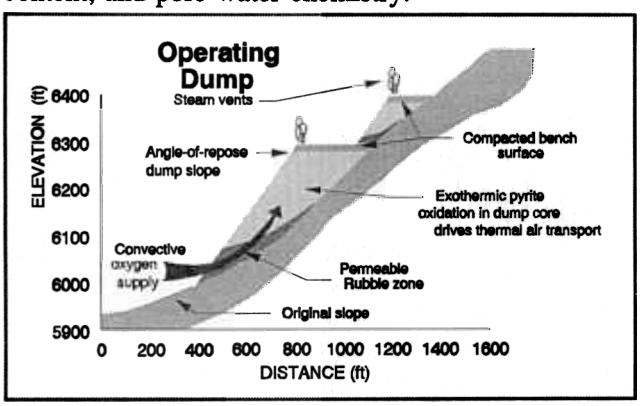

Figure 1. Characteristics of an operating high sulfide dump.

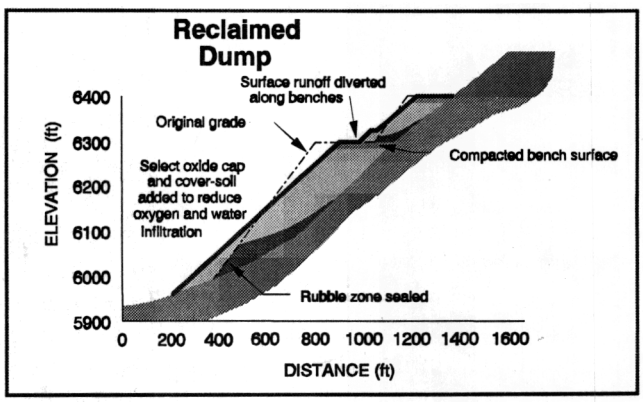

Figure 2. Reclaimed waste rock dump showing placement of soil cover and sealing of the rubble zone.

Methods

A large portion of the northwest dump complex at the Golden Sunlight Mine was regraded in 1991. Approximately 60 cm of oxidized waste rock and 50 cm of cover-soil were placed over the 2:1 regraded slopes. A mixture of dryland grasses and forbs were seeded in spring 1992. Monitoring installations were placed near the crest (site 1) and toe (site 3) of the reclaimed slope (section A-A' in Figs. 3 and 4). In addition, monitoring devices were installed on a prominent reclaimed bench (site 2) designed to direct runoff off the regraded slope. Similar monitoring devices were installed on the bench (site 6) and toe (site 7) of an unreclaimed angle-of-repose dump (section C-C', Figs. 3 and 4).

A climate station was installed at site 2 to provide daily rainfall and temperature data. Downhole devices included thermistors, heat dissipation units, neutron probe access tubes, gas sampling ports, and pore water samplers. Due to the cost of drilling in waste rock, most installations involved multiple-depth completion in the same hole. Neutron probe access tubes consisted of core steel augered into the waste rock. This installation technique maintained close contact with waste material to facilitate water content measurement. Gas-sampling ports were staggered throughout the depth of waste rock (Figs. 5 and 6) which varied from 40 to 170 feet. Shallow pore water samplers installed at depth of 3, 5 and 10 ft consisted of Soil Moisture model 1920 ceramic tip pressure-vacuum lysimeters. Lysimeters installed near the base of the dump (at over 100 ft) were BAT lysimeters which are more suitable for sample recovery from greater depths.

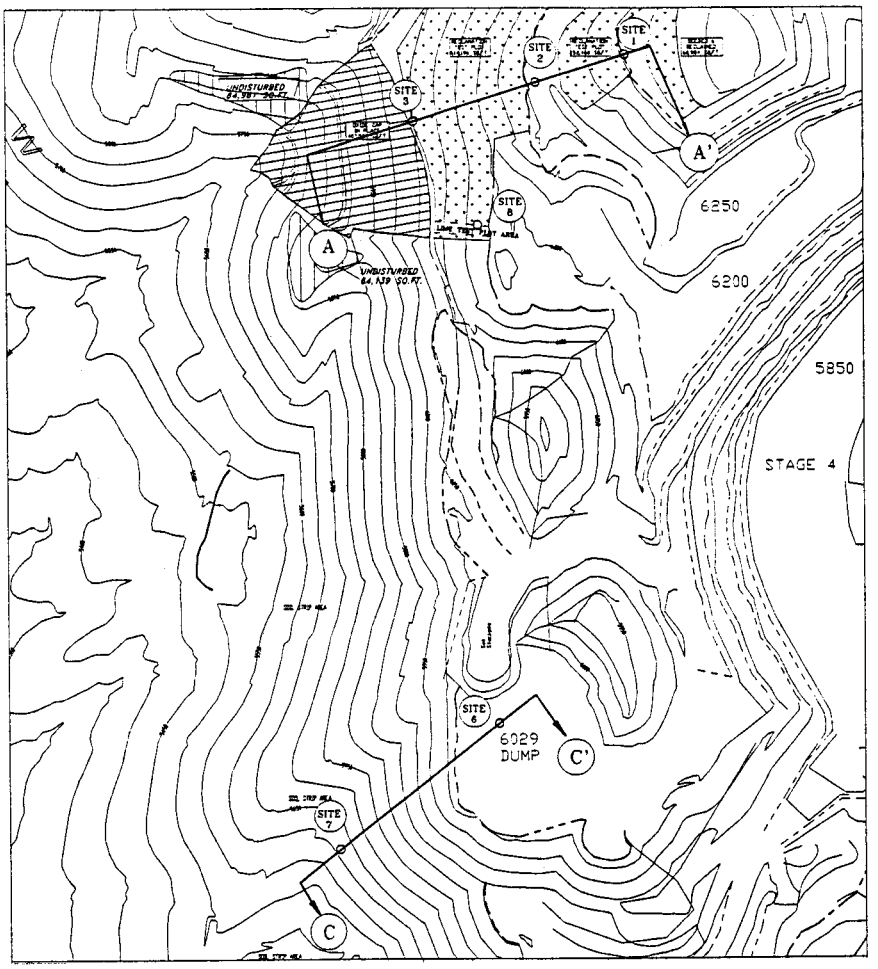

Figure 3. Plan view of Golden Sunlight Mine northwest dump showing reclaimed (north) and unreclaimed (south) test dumps.

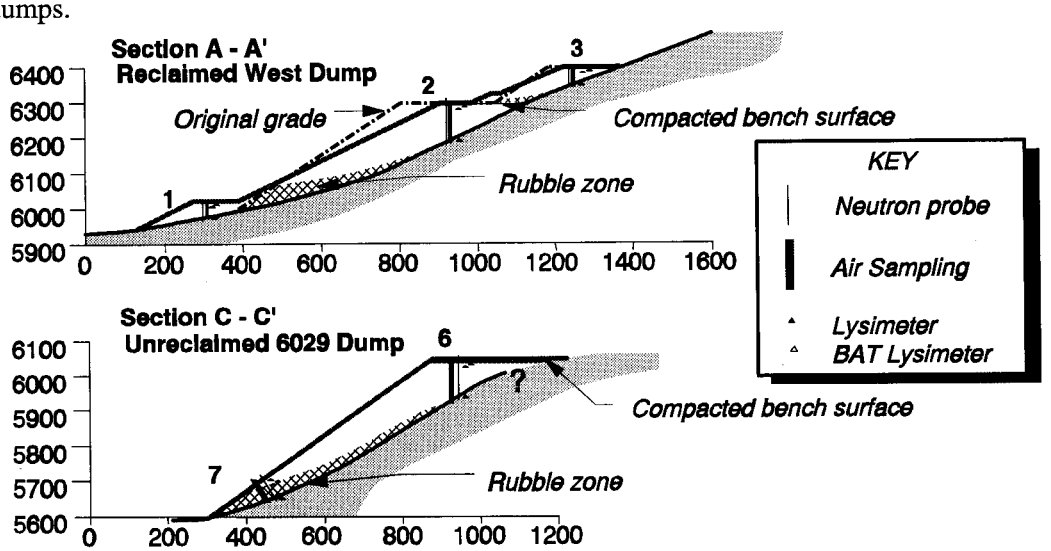

Figure 4. Cross-section view of monitoring devices installed in the northwest dump.

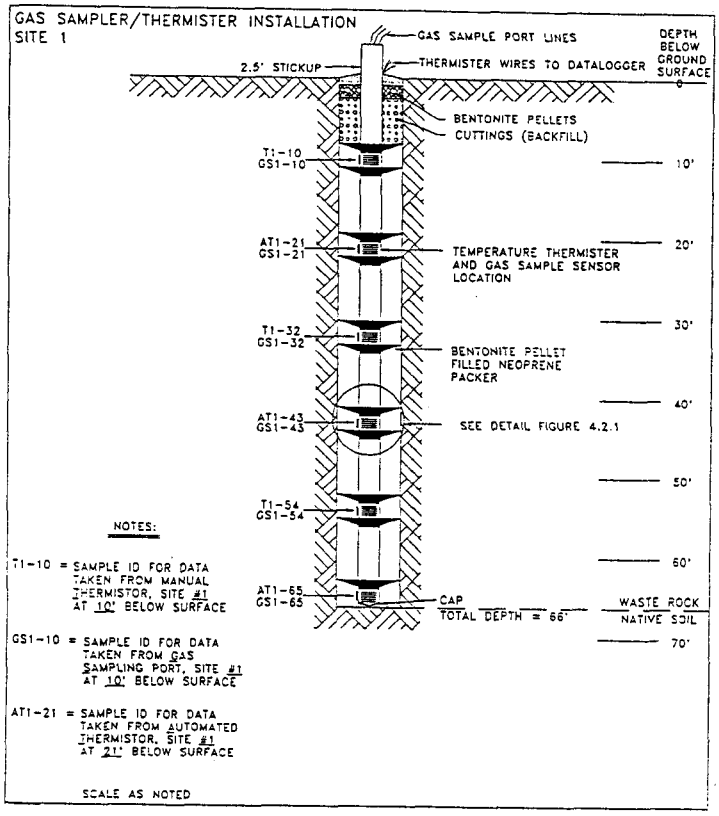

Figure 5. Typical multiple completion gas port assembly for site 1 in the reclaimed section of the Golden Sunlight Northwest Dump.

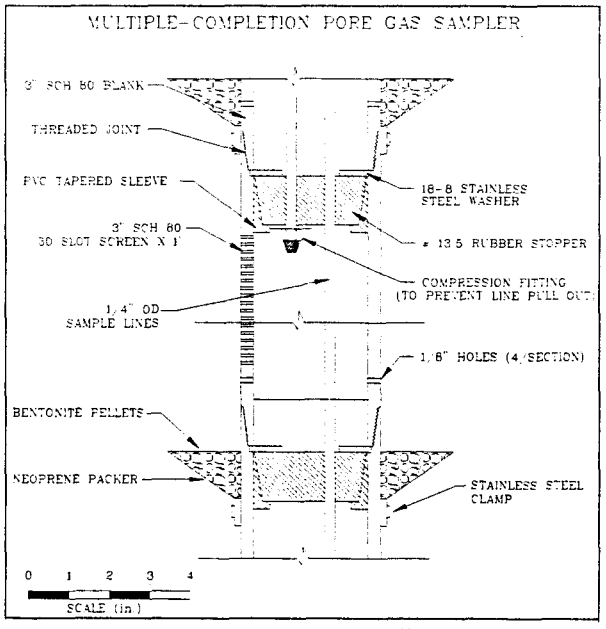

Figure 6. Detail of gas sampling port.

Routine monitoring of temperature, water content, oxygen levels, soil suction levels, and pore water chemistry began in mid-1992. The purpose of the hydrologic monitoring program was to identify differences in oxygen supply, water flux, and pore water chemistry in reclaimed and unreclaimed dumps.

Results

Water Content and Water Balance

Water content in waste rock at the Golden Sunlight Mine is a function of the average rock particle size, and prior saturation by rainfall infiltration. During placement, freshly shot waste rock typically has a volumetric water content of less than 6 percent. The rock particle size gradually increases with depth due to gravity sorting in the end-dumping sequence. As a consequence, residual saturation varies between 8 and 12 percent within the dump with residual saturation generally lower near the base of the dump where larger particles are deposited. Overall, the waste rock has a volumetric "wetting requirement" of 3 to 5 percent. Infiltration gradually wets the waste rock from its initial water content to residual saturation or field capacity. The upper 6 to 10 ft of each waste rock bench differs from the remaining waste rock due to vehicle compaction which pulverizes the material. The fines generated cause residual saturation levels to reach 15 to 20 percent. A 100 ft column of waste rock would retain 3 to 5 ft of solution before seepage could migrate out of the pile.

The overall water balance for each monitoring point is presented in Fig. 8. The cumulative precipitation from July 1992 to October 1993 is compared to the cumulative change in water within the vertical extent of the

dump. Essentially all of the incident precipitation appeared to infiltrate into the toe of the unreclaimed waste rock pile (site 7). The wetting front appears to have nearly reached the base of the dump at site 7. Both the reclaimed dump bench (site 2) and the crest of the unreclaimed dump (site 6) gained far more water than the cumulative rainfall. This apparent anomaly is probably due to run-on from natural hillslopes upgradient of the dump and lateral seepage along the dump foundation. The reclaimed 6300 bench (site 2) was located in a depression which collected a significant amount of runoff water from the 6400 slope in both 1992 and 1993. The control crest location appeared to decrease in water content between spring and late summer of 1993. This change in water content may represent flux of water below the base of the dump.

Both site 1 and site 3, the crest and toe of the reclaimed dump, exhibited a greatly reduced intake of water, averaging about 30 to 40 percent of the incident precipitation. As vegetation becomes better established, the performance of the revegetated soil cap in reducing infiltration is expected to improve. Rainfall received during 1993 was approximately double the long-term average rainfall at the site.

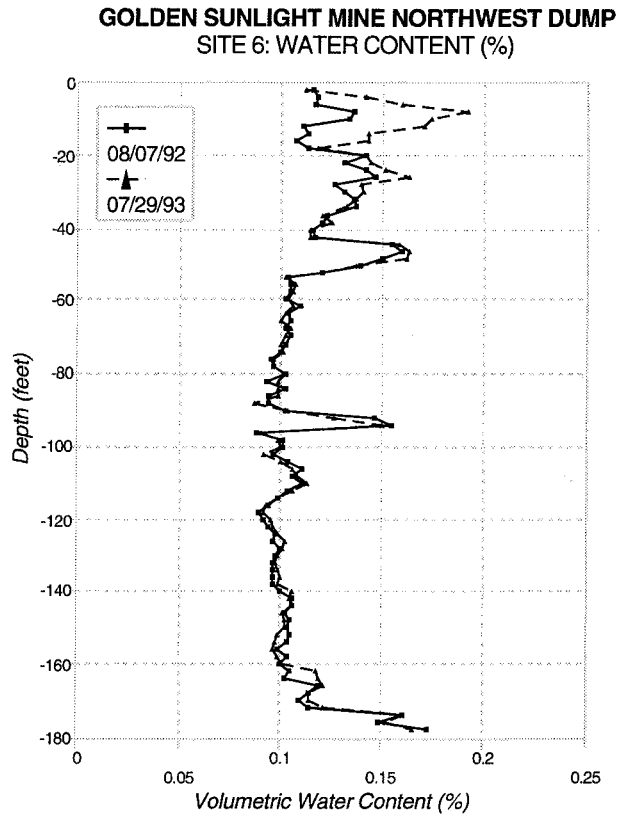

Figure 7. Water content variation with depth in the untreated dump crest. Natural soils were encountered at 175 feet.

Suction Levels

Heat dissipation units are automated devices used to measure soil water potential in soils. A data-logger is used to measure soil suction levels hourly. Long-term trends in suction at site 1 (Fig. 9) corroborated the soil water content data. The base of the dump remained extremely dry at the end of 1993 (water potential <-10 bars) because the wetting front had not reached this level. Soil water potential at 3, 5 and 10 feet generally ranged from -0.6 to -0.3 bars indicating that materials are at residual saturation at these depths. Minor increases in water potential occurred in response to rainfall events.

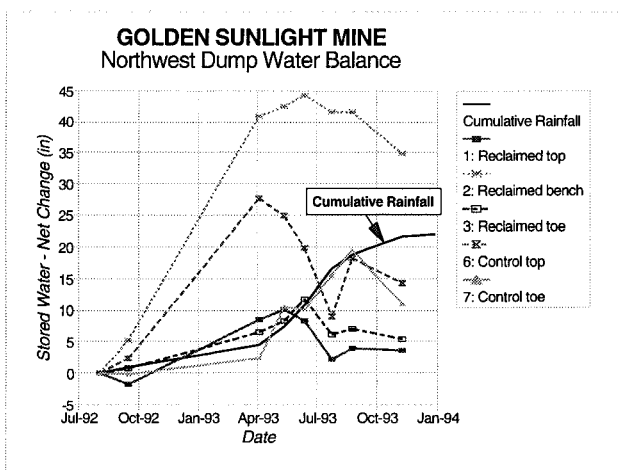

Figure 8. Site water balance for the reclaimed and unreclaimed Northwest Dumps.

Temperature

Temperature is particularly important in this investigation because pyrite oxidation is strongly exothermic. Hence, elevated temperatures provide a direct indication of the spatial extent of microbial pyrite oxidation. Temperature trends for numerous measurement depths at each site are presented in Fig. 10. Site 1 does not indicate significant pyrite oxidation. Temperatures average 8°C, the average annual air temperature. Seasonal temperature fluctuation is only pronounced at the three foot depth. Pyrite oxidation has been triggered between 40 and 75 feet at site 2, the reclaimed 6300 bench. Interestingly, heating is confined to the wetting front which has moved from 40 to 80 feet during the two years of monitoring. It appears that dry waste rock placed at water content below residual saturation (less than about 10%) may be too dry to support *Thiobacillus ferrooxidans* activity. Similarly, the upper 10 feet of the unreclaimed crest is just beginning to heat, and the 33 foot depth which was wetted in mid 1993 may be beginning to heat. The toe of the angle of repose dump had extremely cold temperatures indicative of cold air drainage within the pile. Water content measurements indicated that a large mass of ice developed at this location and melted in late summer.

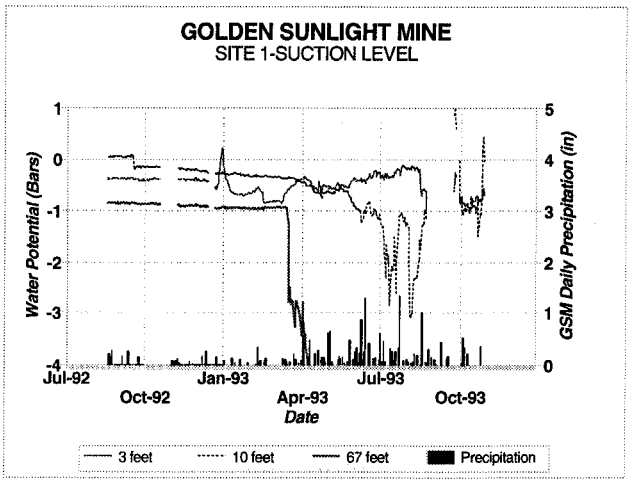

Figure 9. Seasonal variation in soil suction beneath the crest of the reclaimed dump.

Oxygen Levels in Waste Rock Pore Space

Oxygen concentrations were highly elevated at all depths in the reclaimed and unreclaimed waste rock at Golden Sunlight (Fig. 11). Minor decreases in O_2 were noted near the surface of reclaimed sites during the 1993 growing season. The applied cover-soil layer did not serve as an effective oxygen diffusion barrier, however. Reduced oxygen levels were only noted at 33 feet at site 2, the depth at which extreme heating was also noted. The high oxygen levels throughout most of the dump could be either attributed to rapid oxygen advection or diffusion rate or to a lack of oxygen consumption. For the drier, lower half of the dump, oxygen demand appears to be slight due to the apparent minor microbial pyrite respiration.

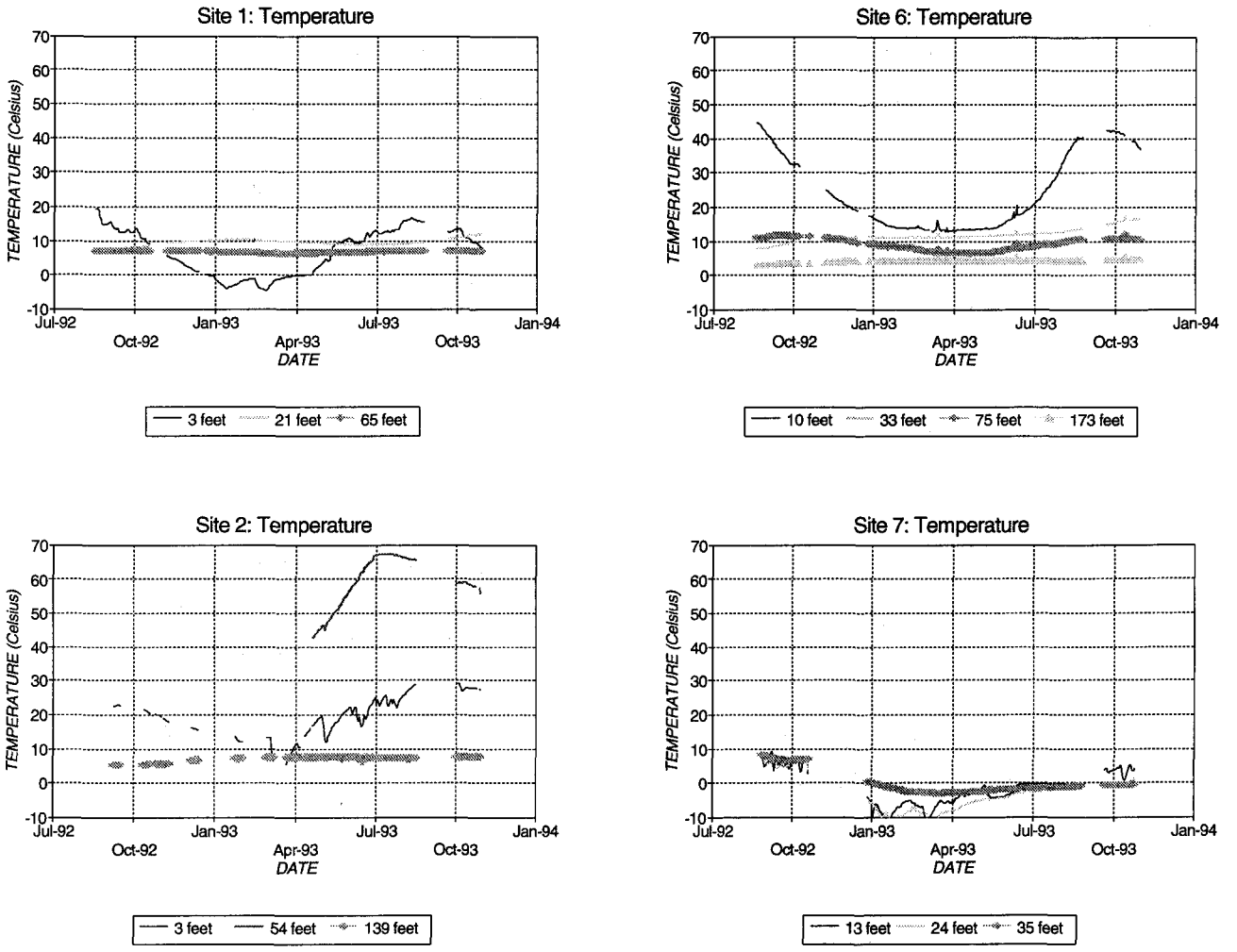

Figure 10. Soil temperatures at reclaimed and unreclaimed monitoring sites.

Pore Water Chemistry

Pore water samples were obtained from 3, 5 and 10 feet in depth at most sites. Samples of pore water could not be obtained from deeper lysimeters placed at the foundation of the dump either due to mechanical damage of the access tube from consolidation or due to very low soil suction levels. In general, pH of pore water ranged from 1.5 to 3 in sulfide waste rock and was from 4 to 7 in oxide waste rock and cover-soil layers.

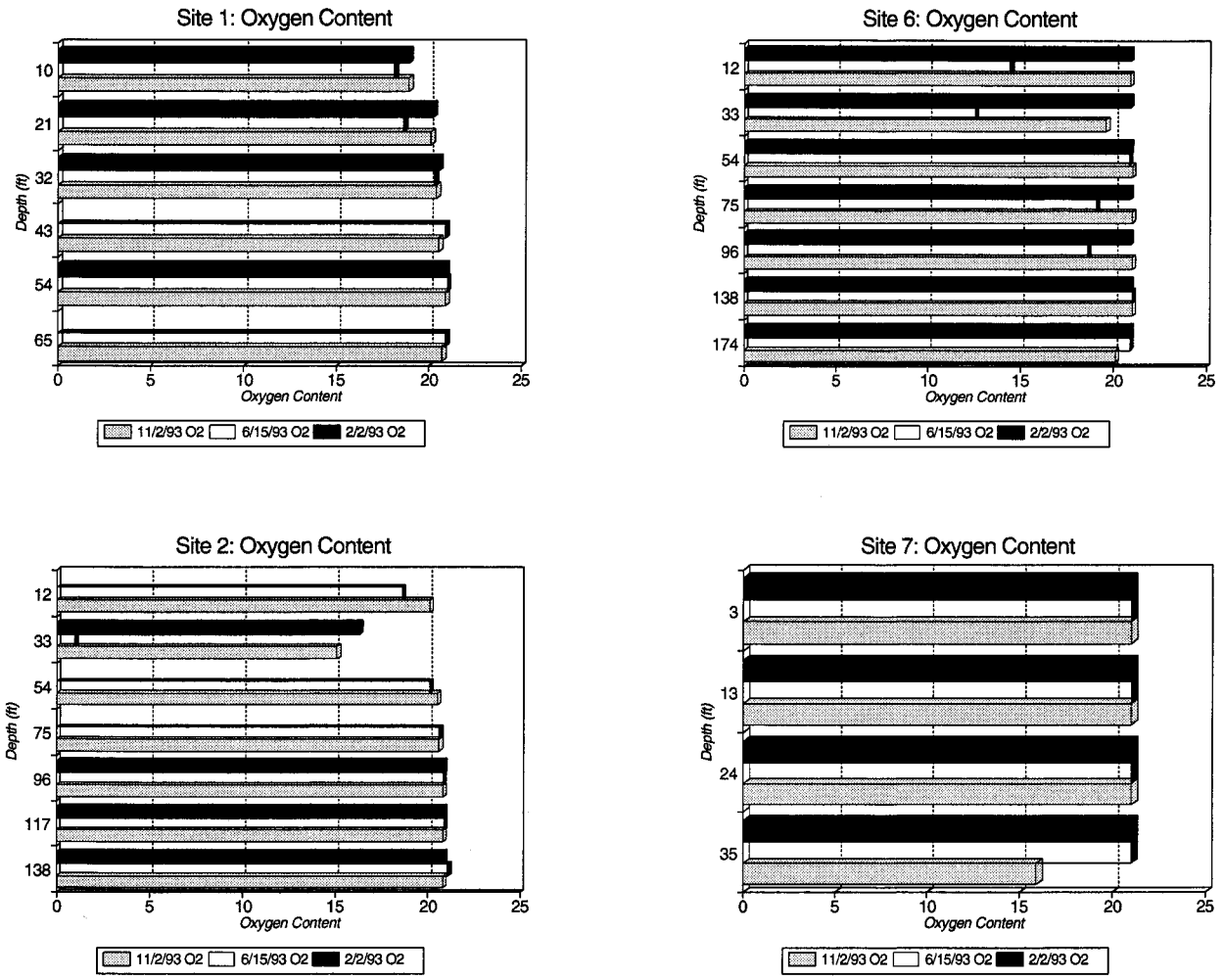

Figure 11. Oxygen levels in pore space at reclaimed and unreclaimed monitoring sites.

Conclusions

Regrading and addition of cover-soil to sulfide waste rock dumps appears to be effective in reducing infiltration of water into the dump. As vegetation becomes established, infiltration may decrease to the point that the rate of migration of the wetting front will be diminished.

Oxidation of pyrite is accompanied by evolution of heat. Although thermally-driven advection was thought to maintain an ample oxygen supply to reactive zones within the dump, the advective cells may be surficial rather than being fed from the coarse-textured dump foundation as originally hypothesized.

Migration of the wetting front, which is currently at around 30 feet through most of the dump, appears to trigger sulfide oxidation. Deeper materials that are relatively dry do not appear to be reacting at present. Pronounced hillslope effects also affect water movement within the dump. Run-on from upgradient areas, and ponding of water on erosion control benches has stimulated deeper water movement in few portions of the Northwest Dump at Golden Sunlight. The practice of concurrent reclamation, that is progressive regrading and revegetation during mining, may be particularly important for sulfide waste rock facilities in semi-arid climates.

Literature Cited

Harries, J.R. and A.I.M. Ritchie. 1987. The effect of rehabilitation on the rate of oxidation of pyrite in a mine waste rock dump. Environ. Geochem Health 9:27-36.

Krauss, Raymond E., 1990. Reclamation Practices at Homestake's McLaughlin Mine. Mining Engineering Nov. 1990(1239-1241).

Schafer, W.M. 1992. Acid-Forming Mining Waste: Prediction, Control and Treatment. pg 345-353 In Randol Gold Forum, Vancouver, B.C., Canada. March, 1992.

COMPARISON OF DULUTH COMPLEX ROCK DISSOLUTION IN THE LABORATORY AND FIELD[1]

Kim A. Lapakko[2]

Abstract: The quality of drainage and the release of sulfate, calcium, and magnesium from five field test piles of Duluth Complex rock with sulfur contents of 0.63% (three piles), 0.79%, and 1.41% were determined for periods of 12 to 14 yr. The pH of drainage from the piles decreased over time and with increasing solid-phase sulfur content. The ultimate drainage pH values for the 0.63% S piles ranged from 4.8 to 5, similar to values observed in the laboratory. Ultimate drainage pH values for sulfur contents of 0.79% (pH 4) and 1.41% (pH 3.5) were about one unit lower than the corresponding laboratory values for these sulfur contents. Over the entire period of record, average rates of sulfate release (2.1 to 10.5 mmol/mt/d) and magnesium release (0.55 to 3.7 mmol/mt/d) increased as the solid-phase sulfur content of the pile increased, while those of calcium release (1.2 to 2.4 mmol/mt/d) were relatively constant with respect to solid-phase sulfur content. Annual release rates for sulfate and calcium were relatively constant over time, while those for magnesium tended to increase over time. Annual release rates for all three parameters increased with increased annual drainage volume, a variable not examined in the laboratory. Release rates in the field were typically 10% to 30% (and in one case, nearly 40%) of those observed in the laboratory. Empirical neutralization potentials in the field decreased as solid-phase sulfur content decreased and were typically 10% to 50% of the corresponding average laboratory values. The empirical neutralization potentials to maintain drainage pH above 6.0 were approximately 0.5% to 8% of ABA NP values for Duluth Complex rock.

Additional key words: acid mine drainage, sulfide mineral oxidation, pyrrhotite, field test, rates.

Introduction

In the mid-1970's AMAX Exploration Inc. was evaluating the potential for developing copper-nickel resources of the Duluth Complex in northeastern Minnesota. At this time little information existed on the potential drainage problems associated with copper-nickel development in Minnesota. The State and AMAX agreed to commence field leaching tests on Duluth Complex rock. AMAX began excavation of a shaft in 1975 and in 1977 constructed six test stockpiles containing lean ore material. Water quality samples were collected periodically from each pile in 1977, and the data were compiled by AMAX Environmental Services Inc. (1978). The test pile studies were conducted from 1978 through the present by the Minnesota Department of Natural Resources (MNDNR), Division of Minerals (Eger and Lapakko 1981, 1985). As part of a cooperative research project with the U. S. Bureau of Mines, the compilation and analysis of data from the test piles were updated through 1991 to aid in development of a dissolution model by the Salt Lake City Research Center. This paper presents data on the quality and quantity of drainage from five of the test piles and the rates of mineral dissolution observed from 1978 through 1991. The period of record for pile 4 was only 5 yr, and these data are not presented. The data are compared with those previously presented on laboratory studies on the dissolution of Duluth Complex rock.

Objectives

The objectives of this paper on the quality of drainage from Duluth Complex rock field test piles are to

1. Describe the variation of drainage quality with respect to solid-phase sulfur content, time, and flow.
2. Determine the rates of sulfate, calcium, and magnesium release.
3. Describe the variation of drainage quality and mass release with respect to sulfur content, time, and flow.

---

[1]Paper presented at the International Land Reclamation and Mine Drainage Conference and the Third International Conference on the Abatement of Acidic Drainage, Pittsburgh, PA, April 24-29, 1994.
[2]Kim A. Lapakko, Principal Engineer, Minnesota Department of Natural Resources, Division of Minerals, St. Paul, MN, USA.

4. Determine the empirical acid neutralization potentials of the Duluth Complex rock samples examined.
5. Compare field results with those generated in the laboratory.

Methods

Climate

Annual precipitation in the study area averages 72.1 cm (Hickok and Associates 1977), and the average watershed runoff is 26.2 cm/yr (Siegel and Ericson 1980). Temperatures are extreme, averaging -14° C in January and 19.1° C in July, with an annual mean of 3.6° C; the ground is covered with snow for an average of 140 days per year (Hickok and Associates 1977).

Test Pile Construction

Materials. Six test stockpiles containing 820 to 1300 metric tons (mt) of low-grade copper-nickel material were constructed in 1977. The piles were approximately 4 m high and 15 m by 25 m at the base. Stockpiles 1 to 4 were constructed of rock mined during the shaft-sinking operation, while piles 5 and 6 contain material from underground drifts. The chemical compositional ranges for the piles are 0.63% to 1.41% S, 0.30% to 0.35% Cu, and 0.083% to 0.085% Ni (table 1). A grab sample was taken from test pile 1 for more extensive chemical and mineralogical analyses (Eger and Lapakko 1981). The major sulfide minerals identified and their volume percentages were pyrrhotite (0.844%), chalcopyrite-cubanite (0.769%), and pentlandite (0.037%). The major silicate minerals and their approximate volume percentages were plagioclase (59%), clinopyroxene (11%), olivine (11%), orthopyroxene (3.7%), and monocrystalline amphibole (3.6%).

Approximately 40% of test pile 4 was removed in 1982 for use in another study of stockpile reclamation techniques (Eger et al. 1984, Lapakko et al. 1986). At this time a representative sample weighing over 3 mt was collected for analysis of particle size distribution, specific surface area, chemistry, and mineralogy. The methods and detailed results of this characterization are presented in Lapakko et al. (1986). The particle size analysis revealed that 11% of the grains were larger than boulder/cobble size classification ($d > 305$mm), 6.8% were boulder/cobble ($76.2 < d \leq 305$ mm), 63% were gravel ($2 < d \leq 76.2$ mm), 15.8% were sand ($0.074 < d \leq 2$ mm), and 4.7% were silt/clay ($0.053 < d \leq 0.105$ mm). The sand, silt, and clay fractions were analyzed for specific surface area, chemistry, and mineralogy. The specific surface area of the fine fractions was roughly inversely proportional to the particle size diameter (table 2). The pH decreased and the sulfide and trace metal content increased with decreasing particle size of the rock. The finer sand, silt, and clay fractions had S, Cu, and Ni contents above the 0.634% S, 0.348% Cu, and 0.083% Ni levels estimated for pile 4 as a whole.

Table 1 Summary of chemical and physical characteristics of test piles

		Pile 1	Pile 2	Pile 3	Pile 6	Pile 5
Date completed				4/20/77		9/10/77
S	%			0.63		1.41
Cu	%			.35		.30
Ni	%			.083		.085
Mass	mt			830		815
Volume	m^3			400		400
Collecting area	m^2			300		340
Surface area .	m^2			430		370
Cover material				Glacial till (coarse sand)		Sandy till over coarse sand
Ave. cover depth	cm	0	23	34	0	54
Vegetated		No	Yes	Yes	No	Yes

Table 2. Characterization of fine fractions from test pile 4.

Size fraction, mm	pH	Total sulfur, %	Sulfide, %	Cu, %	Ni, %	Co, %	Zn, %	Specific surface area, m^2/g
Sand								
0.50 -2.00	6.56	0.67	0.65	0.337	0.062	0.012	0.015	0.60
.177- .50	6.37	.80	.75	.381	.078	.013	.015	.78
.149- .177	6.18	.88	.80	.391	.103	.015	.015	1.1
.105- .149	NA	1.12	1.05	.495	.147	.019	.017	1.6
.075- .105	5.95	1.37	1.30	.585	.221	.022	.019	1.7
Silt and clay								
.053- .075	5.78	1.65	1.57	.647	.253	.024	.019	2.6
<.053	5.77	1.94	1.86	.814	.295	.027	.023	4.7

NA Not available.

X-ray diffraction (XRD) analyses were conducted on the 0.053- to 0.075-mm, the 0.075- to 0.105-mm, and the 0.105- to 0.149-mm size fractions of the rock. Approximately half of this material was plagioclase (with a Na:Ca ratio of about 2:3), and half was a mixture of olivine (with a Fe:Mg ratio of 1:4 to 1:9), pyroxene, and biotite. Lesser amounts of magnetite, amphibole, chlorite, and possibly smectite and/or vermiculite were also identified. The phyllosilicate minerals (biotite, chlorite, smectite, vermiculite) were more common in the finer size fractions.

Piles 1, 3, and 6 were partly covered by plastic at the end of the 1989 field season, for the practical purpose of reducing the volume of drainage the MNDNR is required to treat. The plastic covers were shredded during 1990 by exposure to the elements. A more robust Hypalon cover was placed onto pile 3, thereby terminating flow from this pile at the end of the 1989 field season.

Reclamation Treatments. Three of the piles were left uncovered, as controls, and the remaining three piles were covered (May 1978) with 18 to 29 cm of soil obtained from a nearby borrow pit. Pile 2 was covered with fertile topsoil obtained from the top 30 cm of the borrow pit, while piles 3 and 5 were covered by infertile coarse sand. In 1980 an additional 30 cm of sandy till was added to pile 5. Additional details on vegetation, fertilization, and the application of lime-stabilized sludge to pile 3 (1980, 1982) and a sodium-lauryl-based bactericide to pile 5 (1982) are available in Eger and Lapakko (1981, 1985).

Water Sampling and Analysis. For drainage collection, each pile is underlain by an impervious Hypalon liner (30 mil) which is sloped toward a 15.2-cm perforated plastic pipe. The drainage collected from the piles flows to a common sump. A limited number of water quality samples were collected in 1977, but no flow measurements were made. Since methods in this year deviated from those over the remainder of the study and the data were sparse, the results are not addressed in the text. During 1978, each pile was fitted with a cumulative flow meter and a flow-weighted composite sampler (Eger and Lapakko 1981). For each pump discharge, a fixed volume of sample was placed into the compositing container.

The composite samples were analyzed weekly through 1990 and biweekly subsequently. Samples were filtered through 0.45-μm filters to remove suspended materials prior to analysis. Routine analyses included pH, alkalinity, specific conductance, sulfate, copper, nickel, cobalt, zinc, calcium, and magnesium, although calcium and magnesium were not analyzed in 1983. (Some samples were also analyzed for sodium, potassium, chloride, and dissolved organic carbon.) Specific conductance was analyzed using a Myron L conductivity meter. pH was determined using a Radiometer 29 pH meter from 1978 to 1988, and subsequently using an Orion SA 720 with a

Ross combination electrode (8165). Sulfate was analyzed using the barium sulfate turbidimetric technique (APHA et al. 1992). Metals were analyzed with a Perkin Elmer 603 atomic absorption spectrophotometer.

Calculations

For each period over which composite samples were collected, the mass release was calculated as the product of the concentration in the composite sample and the volume of flow during the period over which the composite was collected. Annual mass release was calculated as the sum of the mass release values for the individual periods for each year. Annual flow-weighted mean concentrations were calculated by dividing the annual mass release by the annual flow. The annual rates of release were calculated as the annual mass release divided by the product of the number of days of flow and the mass of the pile (mt). Average rates of release for the entire period of record were calculated by dividing the total mass release by the number of days of flow.

Empirical neutralization potentials (ENP) were calculated to determine the amount of acid neutralized by the solids prior to the drainage pH decreasing and, for the duration of the period of record, remaining below pH values of 7, 6, 5, 4.5, and 4. The acid neutralized was calculated as the cumulative calcium and magnesium release (expressed as kilograms of $CaCO_3$ per metric ton of rock, or kg/mt $CaCO_3$) prior to the drainage pH decreasing and remaining below the specified pH value. If the drainage pH from a given solid never decreased permanently below a specified value, the ENP was reported as "greater than" the total calcium plus magnesium release for the period of record. Sulfate release was not used for the ENP calculation since some of the sulfate was the product of trace metal sulfide oxidation. The sulfate released from oxidation of copper and nickel sulfides, which comprised 15% to 35% of the sulfide mineral content of the test piles, does not necessarily result in acid production.

Results

Drainage Quality

The test piles typically produced drainage between the middle of March and the middle of November, with an average flow season of 245 days. The pH of drainage from the test piles generally decreased over time, and decreased as the solid-phase sulfur content increased (fig. 1). At the beginning of 1978, the pH of drainage from all piles was between 7 and 8. For the three piles containing 0.63% sulfur, drainage pH decreased gradually from circumneutral to the range of 4.8 to 5.3. The pH of drainage from the piles containing 0.79% and 1.4% sulfur decreased and plateaued within a range of about 0.2 to 0.3 pH unit. The pH of drainage from the 0.79%-sulfur pile decreased until 1982 and subsequently oscillated in the typical range of 4.0 to 4.3. The pH of drainage from the 1.41%-sulfur pile decreased to a lower level, from a median value of 5.5 in 1978 to a typical range of 3.4 to 3.6 from 1979 to 1991. The annual median values actually increased from 1982 (3.40) to 1991 (3.60).

Annual flow-weighted mean sulfate concentrations for the individual piles tended to increase during the first 3 to 4 yr and then oscillated within a fairly constant range, increased as the solid-phase sulfur content increased, and were independent of the annual flow volume. Some deviations from the general trends were observed. Most notably, sulfate concentrations in drainage from the 1.41%-sulfur pile increased to peak levels between 1981 and 1985 and then decreased. From 1987 to 1991 the flow-weighted mean sulfate concentrations from this pile were comparable to, or lower than, those from the 0.79%-sulfur pile. Sulfate concentrations from the 0.79%-sulfur pile increased over time. However, these temporal variations from 1981 through 1991 were relatively small. In general the maximum annual flow-weighted mean sulfate concentrations were typically within a factor of 2 of the minimum value observed during this period.

Annual flow-weighted mean magnesium concentration variations over time were generally parallel to those observed for sulfate and were independent of annual flow volume. Magnesium concentrations were lowest in drainage from the 0.63%-sulfur piles, typically ranging from 2 to 6 mmol/L. The corresponding range for the two piles of higher sulfur content was 7 to 15 mmol/L. For the individual piles, annual flow-weighted mean magnesium

concentrations tended to increase as the annual median pH decreased.

Annual flow-weighted mean calcium concentrations were typically fairly constant, ranging from about 4 to 7 mmol/L. As implied by the constant range, there was little dependence of annual flow-weighted mean calcium concentrations on time of dissolution, sulfur content, or annual flow. The values for the 1.41%-sulfur pile appeared to parallel the decreasing trend observed for sulfate concentrations from 1985 to 1991.

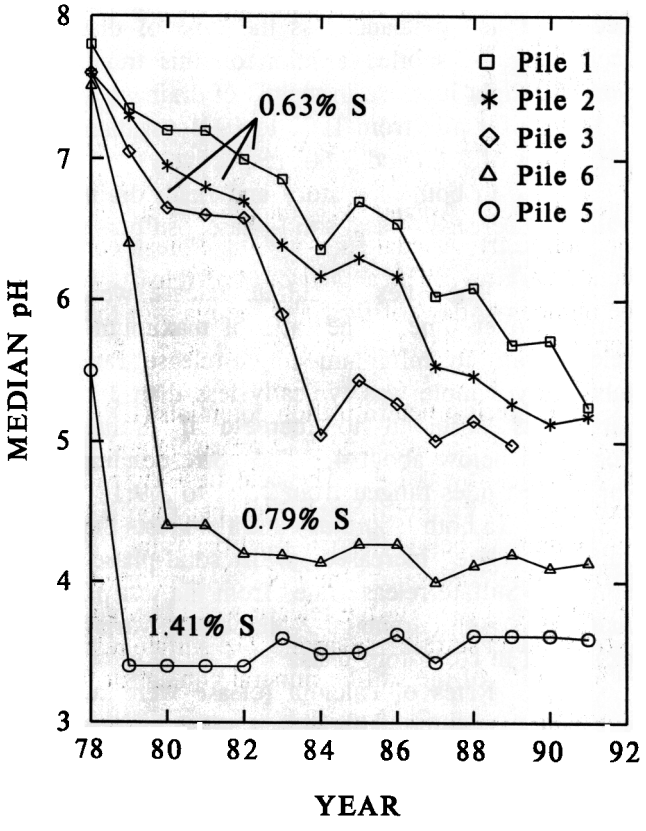

Figure 1. Annual median pH from 1978 to 1991. Drainage pH decreased over time and as solid-phase sulfur content increased.

Annual Rates of Release

The annual rate of sulfate release from each pile oscillated within a fairly constant range (fig. 2). In general, annual sulfate release increased with the solid-phase sulfur content of the pile, although the rates for the 0.79%-sulfur pile were comparable to or exceeded those for the 1.41%-sulfur pile from 1984 to 1991. Sulfate release also increased with annual flow, and temporal variations in the annual rate were largely due to variations in annual flow volume. A graphic example of the flow dependence is the low sulfate-release rate from the 0.79%-sulfur pile in 1990, while the pile was partly covered with plastic. The drainage volume and sulfate mass release were consequently low.

Variations in magnesium release followed similar trends. Similar to the sulfate-release rates from 1984 through 1991, magnesium release from the 0.79%-sulfur pile was usually higher than that from the 1.41%-sulfur pile. In contrast, the annual rates of calcium release typically fell into the range of 1 to 3 mol/mt/d. They did not vary with time or solid-phase sulfur content, but did increase linearly with annual flow.

Empirical Neutralization Potential (ENP)

The pH of drainages from the 0.63%-sulfur rock did not decrease permanently below 5.0. The approximate ranges of ENP values determined for endpoint pH values of 7.0 and 6.0 (ENP_{pH7} and ENP_{pH6}, respectively) were 0.2 to 0.4 and 0.4 to 1.3 kg/mt $CaCO_3$, respectively. The pH of drainage from pile 3 approached 5 at the end of 1989. The 1.3 kg/mt $CaCO_3$ ENP value determined for this pile is assumed to be near the ENP_{pH5} for this pile. The lowest ENP endpoint pH values for the piles with sulfur contents of 0.79% and 1.41% were pH 4.5 and pH 4.0, respectively. The ENP values for any pH value tended to decrease as sulfur content increased.

Comparison of Field and Laboratory Data

Certain qualitative similarities were apparent between the field data and laboratory data (Lapakko 1988, Lapakko and Antonson 1993).

1. Drainage pH generally decreased, or decreased and plateaued, as the time of dissolution increased. A subtle variation on this trend was a possible slight increase in the pH of drainage from the 1.41%-sulfur pile from 1982 to 1991 (median annual pH values of 3.40 and 3.60, respectively).

2. In both laboratory and field, drainage pH values decreased as solid-phase sulfur content increased.

3. The rates of sulfate release were fairly constant over time. The ratio of maximum-sulfate-release rate to minimum-sulfate-release rate for a laboratory sample was typically less than 3:1. This ratio was observed to increase if drainage pH decreased below about 4. The corresponding ratios for the test piles ranged from 2.7:1 to 3.9:1.

4. In both laboratory and field tests the rate of sulfate release increased with solid-phase sulfur content. Sulfate release rates from the test piles also increased with drainage volume, a variable not examined in laboratory tests.

5. Rates of calcium release were relatively constant over time, although it must be noted that laboratory data on calcium release are limited.

6. Rates of calcium release were relatively constant with respect to sulfur content. The rates of calcium release from the test piles also increased with drainage volume, a variable not examined in laboratory tests.

7. Rates of magnesium release increased as time increased, although it must be noted that laboratory data on magnesium release are limited.

8. Rates of magnesium release increased as solid-phase sulfur content increased. The rates of magnesium release from the test piles also increased with drainage volume, a variable not examined in laboratory tests.

9. Neutralization potential values were low and decreased with increasing sulfur content.

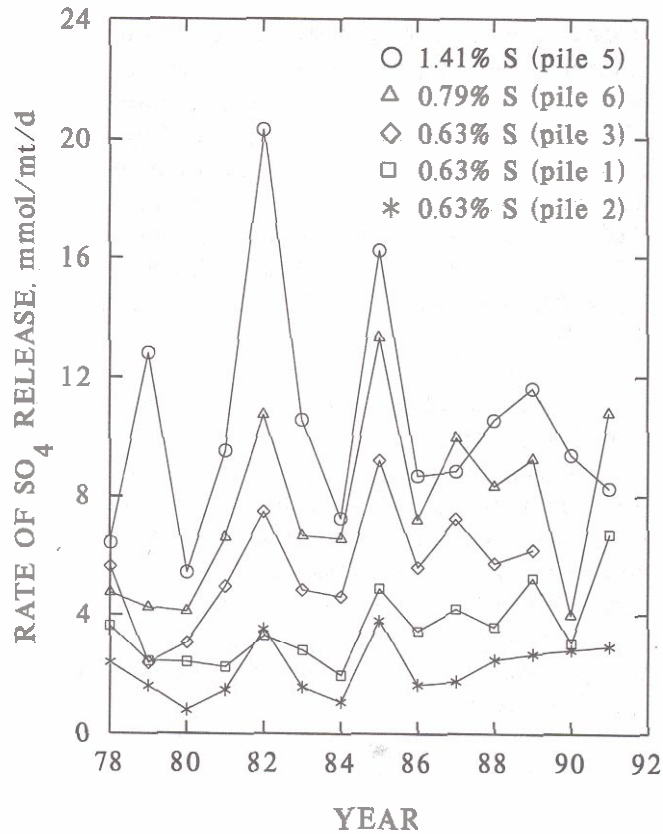

Figure 2. Annual sulfate release rate from 1978 to 1991. Sulfate concentrations generally increased with solid-phase sulfur content and were within a constant range over time.

Field and laboratory data were also quantitatively compared based on drainage pH, neutralization potentials, and rates of release. The minimum drainage pH values observed for the 0.63%-sulfur rock in the field ranged from 4.71 to 4.96 and were reasonably consistent with the laboratory relationship between drainage pH and solid-phase sulfur content. However, the minimum pH values for drainages from the test piles with sulfur contents of 0.79% and 1.41% were about one unit lower than expected based on laboratory data (fig. 3). The minimum pH values observed were typically occasional excursions, and recurrent low pH values were typically 0.1 to 0.2 unit higher.

For the entire period of record, average rates of sulfate release ranged from 2.0 to 10 mmol/mt/d, and increased as sulfur content and drainage volume increased. The average rates of calcium release ranged from 2.1 to 2.4 mmol/mt/d and were fairly constant with respect to sulfur content. Average rates of magnesium release ranged from 0.55 to 3.7 mmol/mt/d and were lowest for the low-sulfur solids and highest for the solids containing 0.79% sulfur.

The rates of sulfate, calcium, and magnesium release observed for the test piles were compared to laboratory rates for the Duluth Complex samples of similar sulfur content (Lapakko and Antonson 1993). The laboratory rates were from the last 15 to 36 weeks of the period of record. The ratios of field rates to laboratory rates, or retardation factors, ranged from 0.053 to 0.46, with most values in the range of about 0.1 to 0.36 (table 3). This indicates that the laboratory rates were roughly 3 to 10 times those in the field.

The neutralization potentials of the test piles were lower than those for laboratory samples, which is consistent with the lower drainage pH levels observed in the field. The ENP values for the 0.63%-sulfur rock were roughly 25% to 50% of those observed for laboratory samples of similar sulfur content (table 4). Although the ENP_{pH6} and ENP_{pH7} values from pile 3 were higher than this range, the ENP_{pH5} value was 46% of the corresponding value for laboratory samples.

The field ENP values for the 0.79%-sulfur rock were 13% to 54% of the corresponding values for laboratory samples of similar sulfur content. The ratios of field to laboratory ENP were lowest for the 1.41%-sulfur rock, typically 5% or less than those determined in the laboratory.

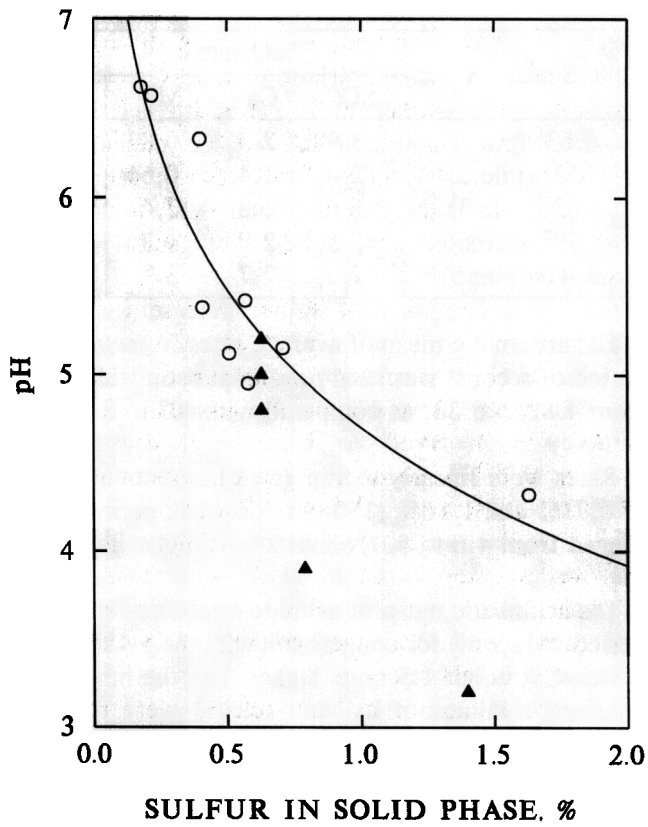

Figure 3. Comparison of recurrent minimum drainage pH in field (▲) and laboratory (○). Laboratory data represents drainage pH after 150 weeks of dissolution of Duluth Complex samples (Lapakko and Antonson 1993).

Discussion

There were several differences between the conditions in the laboratory dissolution experiment and those in the field study. Laboratory particles were smaller than the average particle in the field, ranging from 0.053 mm to 0.149 mm in diameter, and therefore had a higher specific surface area. Due to the relatively uniform particle size, the available mineral surface area was roughly proportional to the amount of the mineral present. In contrast, the fraction of the rock surface area comprised of iron sulfide minerals in the field was most likely higher than that indicated by the sulfur content of 0.63%. Sulfide minerals comprised a disproportionately large fraction of the fine material the field, as indicated by the elevated sulfur content of this fraction (table 2). This material also had the highest specific surface area of the field rock. Therefore, iron sulfide minerals comprised a larger fraction of the field rock surface area than indicated by the sulfur content alone.

Hydrologic differences also existed. The volume of rinse water per unit mass rock yielded approximately 300 L per ton of rock per day of drainage in the laboratory, roughly three orders of magnitude greater than the yields of 0.27 to 0.38 L per ton of rock per day in the field. Furthermore, the flow of the laboratory rinse water through the solids was fairly uniform, whereas preferential flow was probable in the field setting.

Despite these differences there were numerous similarities between the field and laboratory results. As cited earlier, the variations of drainage pH and chemical mass release were qualitatively comparable in the two settings.

Table 3. Comparison of field and laboratory release rates. Rates in moles per gram rock per second x 10^{-14}.

Sulfur, %	Field rate			Lab rates			Retardation factor			
	SO_4	Ca	Mg	SO_4	Ca	Mg	SO_4	Ca	Mg	Ave.
0.63[1] (pile 1)	3.9	2.5	0.86	[1]25	[1]6.7	[1]12	0.16	0.37	0.072	0.20
.63[1] (pile 2)	2.4	1.4	0.64	25	6.7	12	0.096	0.21	0.053	0.12
.63[1] (pile 3)	6.4	2.8	2.4	25	6.7	12	0.26	0.42	0.20	0.29
.79[2] (pile 6)	8.5	2.8	4.3	[2]26	[2]6.1	[2]12	0.33	0.46	0.36	0.38
1.41[3] (pile 5)	12	2.7	3.7	[3]66	[3]19	[3]21	0.18	0.14	0.18	0.17

[1] The arithmetic mean of average rates from samples with sulfur contents of 0.57%, 0.58%, and 0.71% (150 week period of record) was used for comparison with 0.63%-sulfur rock. Minimum pH values for these samples ranged from 4.82 to 5.38, as compared with 4.7 to 5.0 in the field.

[2] Rates were linearly extrapolated based on sulfur content using average rates from samples with sulfur contents of 0.71% and 1.16% (150- and 69-week periods of record, respectively). Minimum pH values for these samples ranged from 4.6 to 5.0, about 1 unit higher than the pH 3.7 minimum value for the field pile.

[3] The arithmetic mean of average rates from samples with sulfur contents of 1.40% and 1.44% was used (69-week period of record) for comparison with the 1.41%-sulfur pile. Minimum drainage pH for these samples ranged from 4.4 to 4.9, about 1.5 units higher than the minimum drainage pH for the field pile and and 1 unit higher than its recurrent minimum pH.

Table 4. Comparison of field and laboratory neutralization potentials.

S, %	pH 7	pH 6	pH 5	pH 4.5	pH 4	pH 3.5
FIELD NEUTRALIZATION POTENTIAL[1]						
0.63 (pile 1)	0.346	0.781	>1.059	>1.059	>1.059	>1.059
.63 (pile 2)	.179	.393	>.642	>.642	>.642	>.642
.63 (pile 3)	.442	1.254	>1.340	>1.340	>1.340	>1.340
.79 (pile 6)	.157	.172	.226	1.702	>2.074	>2.074
1.41 (pile 5)	.044	.044	.096	.130	.136	>1.889
RATIO OF FIELD ENP TO LABORATORY ENP						
0.63 (pile 1)	0.52	0.52	NAp	NAp	NAp	NAp
.63 (pile 2)	.27	.26	NAp	NAp	NAp	NAp
.63 (pile 3)	.66	.84	NAp	NAp	NAp	NAp
.79 (pile 6)	.54	.23	0.13	NAp	NAp	NAp
1.41 (pile 5)	.17	.056	<.056	<0.045	<0.044	NAp

[1] kg/mt $CaCO_3$
NAp Not applicable.

Quantitatively, the drainage from 0.63-percent sulfur rock in the laboratory approximated that in the field. However, pH of field drainages from the 0.79%- and 1.4%-sulfur rock were about 1 and 1.5 units, respectively, lower than the corresponding laboratory values. These field drainage pH values may have been lower due to a higher iron sulfide surface area than indicated by the sulfur content alone. The low rinse water to rock ratio in the field would also lend to increased H^+ concentrations.

Both the rates of mineral dissolution and subsequent reaction product transport probably contributed to the lower sulfate, calcium, and magnesium release rates (per unit mass) observed in the field. First, the larger field particles have a lower specific surface area (surface area per unit mass) than the smaller particles used in the laboratory. The lower surface area in the field would retard the sulfate, calcium, and magnesium release per unit mass rock, since both sulfide mineral oxidation and silicate mineral dissolution are surface reactions. The reaction environment in the field, where temperatures are colder, may also retard reaction rates. Limitation of sulfide oxidation by oxygen transport seems unlikely due to the small test pile size.

Limited transport of reaction products in the field also may have reduced rates of release. Hydrologic variables, which were not influential in the laboratory, could have contributed to this transport limitation. The relatively low flow in the field may have limited transport. This is supported by the observation that release rates in the field increased with flow. Preferential flow would limit the transport of reaction products from some rock surfaces. This would essentially reduce the amount of rock in the test piles that was actually contributing to the observed chemical release. The degree of transport in the field may also be limited by chemical precipitation of dissolution reaction products. In particular, the formation of gypsum might limit the rates of sulfate and calcium release. Gypsum formation was not a problem in the laboratory since the high rinse-water-to-solid ratio produced relatively low concentrations of sulfate and calcium in the drainages.

In addition to the larger particle size in the field, the low field ENP values may have been influenced by factors similar to those discussed regarding drainage pH. First, preferential flow in the field piles would reduce the amount of silicate minerals, which could contribute to acid neutralization. For example, if flow through the pile contacted only half the silicate minerals, the observed neutralization potential of the rock would be half the actual value for the entire pile. Second, if the fraction of rock surface area comprised of silicate minerals in the laboratory samples exceeded that in the test piles, the laboratory solids would be expected to neutralize acid more efficiently. Third, the ratio of available reactive surface area of sulfide minerals to that of silicate minerals present in the test pile rock may have been greater than that in the laboratory. This would be equivalent to increasing the sulfur content of rock in the laboratory. As was observed in the laboratory, neutralization potential tended to decrease as sulfur content increased.

More rigorous analysis of the recently compiled laboratory and field data is presently in progress at the Minnesota Department of Natural Resources. The data are also being used to aid development of a geochemical predictive model for acid mine drainage at the US Bureau of Mines Salt Lake City Research Center.

Acknowledgments

The test piles were constructed by AMAX Exploration Inc. Sulfate was analyzed by Jean Matthew, while calcium and magnesium were analyzed by Albert Klaysmat at the Hibbing office of the Minnesota Department of Natural Resources. Since 1978 sampling and sampling maintenance have been the responsibility of several people: Bruce Johnson, Anne Jagunich, and, most recently, Cal Jokela and David Antonson. Paul Eger has supervised these activities. Jon Wagner provided much of the data input and Jim Porter was responsible for the most recent data management, as well as tabular and graphical output. The U. S. Bureau of Mines provided funding to support data compilation and analysis as part of Cooperative Agreement C0219003.

References

AMAX Environmental Services Inc. 1978. The field leaching summary report, 1977, Minnamax project. AMAX Exploration Inc. Denver CO.

American Public Health Association, American Water Works Association, Water Environment Federation. 1992. Standard methods for the examination of water and wastewater, 18th Edition, American Public Health Association, Washington, DC.

Eger, P. and K. A. Lapakko. 1981. The leaching and reclamation of low-grade mineralized stockpiles. p. 157-166. In Proceedings 1981 Symposium on Surface Mining Hydrology, Sedimentology and Reclamation. (Lexington, KY, December 7-11, 1981).

Eger, P. and K. A. Lapakko. 1985. Heavy metals study: Progress report on the field leaching and reclamation program: 1977-1983. MN Dept. Nat. Resour., Division of Minerals, St. Paul, MN. 53 p.

Eger, P., K. A. Lapakko, and P. G. Chamberlain. 1984. Mixed disposal of waste rock and tailings to reduce trace metal release from waste rock. p. 49-56. In Proceedings 1984 Symposium on Surface Mining Hydrology, Sedimentology, and Reclamation. OES Publications, College of Engineering, Univ. KY, Lexington, KY.

Hickok and Associates. 1977. Water resources investigation for the possible MINNAMAX mining facility Minneapolis, MN. 96 p.

Lapakko, K. A. 1988. Prediction of acid mine drainage from Duluth Complex mining wastes in northeastern Minnesota. p. 180-190. In Mine Drainage and Surface Mine Reclamation. v. 1. Mine Water and Mine Waste. Proceedings 1988 Mine Drainage and Surface Mine Reclamation Conference. BuMines IC 9183.

Lapakko, K. A. and D. A. Antonson. 1993. Oxidation of sulfide minerals present in Duluth Complex rock: A laboratory study. p. 593-607. In Environmental geochemistry of sulfide oxidation. ACS Symposium Series No. 550, American Chemical Society, Washington, DC.

Lapakko, K. A., P. Eger, and J. D. Strudell. 1986. Low-cost removal of trace metals from copper-nickel mine drainage. Final report, BuMines Contract J0205047, NTIS#PB 87-186136. 103 p.

Siegel, D. I. and D. W. Ericson. 1980. Hydrology and water quality of the copper-nickel study region, northeastern Minnesota. U.S. Geol. Surv., Water Resour. Inv. 80-739, Open file report.

ACID-NEUTRALIZATION REACTIONS IN INACTIVE MINE TAILINGS IMPOUNDMENTS AND THEIR EFFECT ON THE TRANSPORT OF DISSOLVED METALS[1]

David W. Blowes[2], Carol J. Ptacek[3], Emil O. Frind[2],
Raymond H. Johnson[2], William D. Robertson[2], and John W. Molson[2]

Abstract: The H^+ generated by sulfide oxidation in inactive mine wastes is consumed by a series of mineral-dissolution reactions. Previous studies conducted at the Nordic uranium tailings impoundment near Elliot Lake, ON, indicated these H^+-consuming reactions occur in a stepwise sequence: calcite dissolution, siderite dissolution, $Al(OH)_3$ dissolution and $Fe(OH)_3$ dissolution. Similar series of acid neutralization reactions have been observed at tailings impoundments at the Heath Steele Zn-Pb mine, NB, the Waite Amulet Cu-Zn mine, Noranda, QC, the Delnite Au mine, Timmins, ON, and the Copper Cliff and Nickel Rim Ni-mines, Sudbury, ON. At all of these locations, near-equilibrium conditions, as indicated by geochemical modelling conducted using MINTEQA2 or PHRQPITZ, are attained with respect to similar sequences of pH-buffering phases. These acid-neutralization reactions have a strong effect on the transport of dissolved metals. Calculations conducted using the 2-D coupled solute-transport/geochemical mass-transfer model MINTRAN predict pH buffering sequences and metal attenuation mechanisms that are similar to those observed at the field sites. Model simulations suggest that some pH-sensitive metals should be retained within the tailings or underlying aquifers.

Additional Key Words: acid-neutralization, tailings, metals, solute-transport modelling, groundwater, aquifers

Introduction

Acid-neutralization processes are fundamental in controlling the environmental effects of wastes from base- and precious-metal mines. In mine tailings impoundments, the balance between H^+-generating sulfide-oxidation reactions and H^+-consuming mineral-dissolution reactions controls the pH at the location of sulfide oxidation and at locations downgradient along the groundwater flow path. Buffering reactions that control the pH near the location of sulfide oxidation affect the rate of sulfide oxidation and the release of dissolved Fe^{2+} and other metals to the tailings pore water. Buffering reactions that occur along the groundwater flow path affect the mobility of dissolved metals as they are transported through the mine wastes and through underlying geologic materials. Tailings impoundments are characterized by a large number of dissolved constituents and a large quantity of tailings solids, all contributing to the chemical evolution of the tailings pore water. The extent of pH buffering depends on the mass of acid-consuming minerals and on the mineralogy of these materials.

The importance of acid-neutralization reactions in mine wastes has been recognized for several decades, as has the benefit of attaining a balance between acid generation and acid neutralization. In response to the need to predict the potential for release of acid drainage from mine wastes, a series of predictive tests and acid-base accounting procedures has been developed (e.g. Ferguson and Erickson 1987). The objective of acid-base accounting procedures and acid-generation predictive tests is to assess the potential for a given mine waste to generate acid.

---

[1]Paper presented at the International Land Reclamation and Mine Drainage Conference and the Third International Conference on the Abatement of Acidic Drainage, Pittsburgh, PA, April 24-29, 1994.

[2]David W. Blowes, Assistant Professor, Emil O. Frind, Professor, Raymond H. Johnson, M.Sc. Graduate, William D. Robertson, Research Assistant Professor, and John W. Molson, Research Associate, Waterloo Centre for Groundwater Research, University of Waterloo, Waterloo, ON, Canada.

[3]Carol J. Ptacek, Research Scientist, Environment Canada, Burlington, ON, Canada.

The results of field studies indicate that acid neutralization in mine wastes and underlying aquifers occurs through a complex series of reactions (Smyth 1981; Morin 1983; Dubrovsky 1986; Morin et al. 1988). It is necessary to investigate the benefits and effects of these pH-buffering reactions because of the variety of metal-bearing sulfide minerals present in base- and precious-metal tailings impoundments and because the mobilities of many of the metals derived from oxidation of these sulfide minerals varies with changing pH.

Acid Generation in Mine Wastes

The principal reactions that generate H^+ are the oxidation of sulfide minerals, the oxidation of Fe^{2+} and hydrolysis of Fe^{3+}, and the precipitation of metal hydroxide and hydroxysulfate phases. The most common sulfide minerals in base- and precious-metal mine tailings are pyrite (FeS_2) and pyrrhotite ($Fe_{(1-x)}S$). The oxidation of pyrite produces two moles of H^+ for each mole of pyrite oxidized through the reaction:

$$FeS_2 + \frac{7}{2}O_2 + H_2O \rightarrow Fe^{2+} + 2SO_4^{2-} + 2H^+ \tag{1}$$

Subsequent oxidation of Fe^{2+} and hydrolysis and precipitation of $Fe(OH)_3$ produces an additional two moles of H^+ resulting in the overall reaction:

$$FeS_2 + \frac{15}{4}O_2 + \frac{7}{2}H_2O \rightarrow Fe(OH)_3 + 2SO_4^{2-} + 4H^+ \tag{2}$$

The precipitation of other Fe(III)-bearing phases, such as goethite (α-FeOOH) or schwertmannite ($Fe_8O_8(OH)_6SO_4$) (Bigham et al. 1990), may occur, releasing differing amounts of H^+. Alternatively, Fe^{3+} may be consumed through further oxidation of sulfide minerals, e.g.

$$FeS_2 + 14Fe^{3+} + 8H_2O \rightarrow 15Fe^{2+} + 2SO_4^{2-} + 16H^+ \tag{3}$$

In many tailings impoundments, particularly those resulting from the concentration and recovery of nickel, pyrrhotite is the most abundant sulfide mineral. Oxidation of pyrrhotite may proceed to completion through the reaction:

$$Fe_{(1-x)}S + (2-\frac{x}{2})O_2 + xH_2O \rightarrow (1-x)Fe^{2+} + SO_4^{2-} + 2xH^+ \tag{4}$$

or may proceed to partial completion, generating Fe^{2+} and elemental S^0 through the reaction:

$$Fe_{(1-x)}S + (2-2x)Fe^{3+} \rightarrow (3-3x)Fe^{2+} + S^0 \tag{5}$$

This elemental S^0 may be subsequently oxidized to SO_4^{2-}. Partial oxidation of pyrrhotite, resulting in accumulation of S^0, has been observed at two Ni mine-tailings impoundments (Coggans et al. 1994; Jambor and Owens 1993), and at an inactive Cu-Zn mine-tailings impoundment (Jambor 1987; Blowes and Jambor 1990).

The zone of active sulfide oxidation in most tailings impoundments is limited to the vadose zone, near the tailings surface, where oxygen transport by gas-phase diffusion is rapid. In this zone, the weathering of sulfide minerals may be complete (reaction 2), resulting in the formation of stable secondary precipitates such as goethite, or incomplete, with some of the Fe derived from the initial sulfide remaining in solution as dissolved Fe^{2+} (reaction

1). Ferrous iron-bearing sulfate and hydroxide minerals are relatively soluble. As a result, dissolved Fe^{2+} concentrations contained in tailings pore waters may be high (up to 70 g/L; Blowes et al. 1991). This dissolved Fe^{2+} is displaced along groundwater flow paths and ultimately discharged to the surface water flow system where oxidation to Fe^{3+} and precipitation of ferric oxyhydroxide phases result in the generation of H^+ in the surface-water flow system (Dubrovsky et al. 1984a; Coggans et al. 1994).

Table 1. Principal pH-buffering phases in mine tailings impoundments.

Mineral	Formula
Calcite	$CaCO_3$
Dolomite	$CaMg(CO_3)_2$
Siderite	$FeCO_3$
Mixed carbonates	$(Ca,Mg,Fe,Mn)CO_3$
Gibbsite[1]	$Al(OH)_3$
Ferrihydrite[1]	$Fe(OH)_3$
Goethite	α-FeOOH
K-Jarosite	$KFe_3(SO_4)_2(OH)_6$
Aluminosilicates	

[1]or equivalent amorphous phase

Acid Neutralization in Mine Wastes

The principal acid-neutralization mechanisms in inactive mine tailings impoundments are carbonate mineral dissolution, hydroxide mineral dissolution, and aluminosilicate mineral dissolution (table 1). Unlike sulfide-oxidation reactions, many acid-neutralization reactions are independent of gas-phase O_2 concentration. Acid-neutralization reactions can occur along the groundwater flow path throughout the tailings impoundment and in underlying aquifers, limited only by the availability of acid-consuming mineral phases. These H^+-consuming reactions result in the general increase in pH with increasing depth that is observed at many tailings impoundments (fig. 1; Dubrovsky et al. 1984a; Morin et al. 1988; Blowes and Jambor 1990; Blowes et al. 1991; Coggans et al. 1994). Consequently, the water present near the base of tailings impoundments, or present in aquifers underlying the tailings impoundment, is usually near-neutral in pH, but may contain high concentrations of acid-generating Fe^{2+}.

Acid-consuming reactions affect both the rate of sulfide oxidation and the distribution of sulfide-oxidation products between the tailings pore water and solid-phase precipitates. Numerous studies have concluded that the rate of sulfide oxidation in mine waste piles and heap-leach systems is controlled by the supply of oxidant to the mineral surface (Cathles 1979; Davis and Ritchie 1986; Nicholson et al. 1990). Processes limiting the supply of oxidant are transport through the mine waste pile to the depth of active oxidation and diffusion of oxidants (O_2 or Fe^{3+}) through oxide coatings that surround unaltered sulfide cores (Davis and Ritchie 1986). Nicholson et al. (1990) concluded that transport of oxygen through alteration rims surrounding pyrite grains controlled the rate of pyrite oxidation in an experimental study conducted under near-neutral pH conditions. In the field, Blowes and Jambor (1990) and Coggans et al. (1994) observed well-developed alteration rims, composed of goethite and jarosite, surrounding sulfide grains under low pH (3.5<pH<4.5) conditions. No alteration rims were observed by Blowes et al. (1994) on sulfide grains present under very low pH conditions (pH<1.5). This pattern suggests that the formation of secondary alteration rims may be a primary control on the rate of sulfide oxidation in all but the most extreme low pH settings.

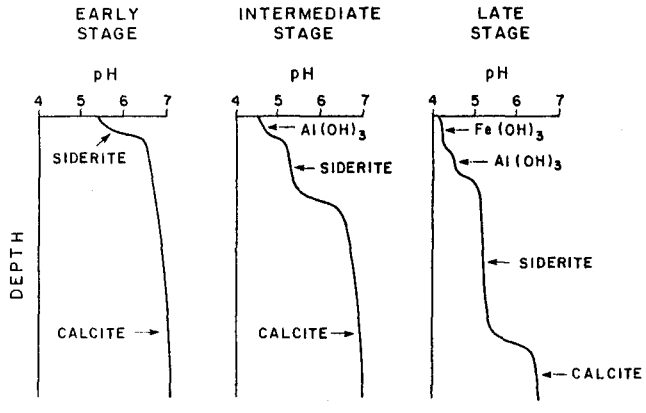

Figure 1. Development of pH-buffering zones during early, intermediate and late stages of sulfide oxidation.

Field observations made at tailings impoundments with similar sulfide contents but varying

carbonate mineral contents suggest that the location of H^+ consumption is important in determining the potential for future acid production. The Nordic U tailings impoundment near Elliot Lake, Ontario, and the Delnite Au tailings impoundment at Timmins, Ontario both contain approximately 5 wt% sulfide minerals, primarily as pyrite. The carbonate content of the Nordic tailings is generally <0.1 wt% as $CaCO_3$, whereas the carbonate content of the Delnite tailings is >20 wt%. At the Nordic site, the pH in the vadose zone is low (1<pH<4) and much of the Fe^{2+} released through pyrite oxidation remains in solution, resulting in pore-water Fe concentrations that exceed 20,000 mg/L at some locations (Dubrovsky et al. 1984b). This water is being displaced down through the tailings and laterally through an underlying aquifer where it is neutralized along the groundwater flow path. Concentrations of dissolved Fe^{2+}, however, remain high along the groundwater flow path. Acidic conditions are generated as this ferrous-rich water discharges to the surface-water flow system downgradient from the tailings impoundment. At the Delnite site, the pH in the vadose zone has remained high (6<pH<8), favoring precipitation of Fe oxyhydroxide minerals, dominantly goethite (Jambor and Blowes 1991). As a result of goethite precipitation, Fe concentrations are generally < 50 mg/L (Blowes 1990). These Fe concentrations represent an acid-generating potential that is less than the acid-consuming potential of the pore-water alkalinity, therefore no acidity is generated as this water is discharged to the surface-water flow system. The importance of maintaining high carbonate contents in the vadose zone of the tailings impoundments is thus illustrated. At both sites, acid-neutralization reactions have produced pore waters near the base of the impoundments that are near neutral in pH, but the high concentrations of dissolved Fe^{2+} in the Nordic pore water represent a high acid-generating potential in contrast to the low acid-generating potential at Delnite.

Sequential pH Buffering Reactions

Field studies conducted in a number of tailings impoundments indicate series of equilibrium pH-buffering reactions controlling the pH of the tailings pore water (Smyth 1981; Dubrovsky et al. 1984a; Blowes and Jambor 1990; Johnson 1993). These series are similar to those which Morin et al. (1988) observed in a plume of tailings-derived water moving outward from beneath the Nordic Main uranium tailings impoundment near Elliot Lake, Ontario, where the sequence follows the order: calcite dissolution, siderite dissolution, $Al(OH)_3$ dissolution and $Fe(OH)_3$ dissolution.

The following example is based on results of a field study conducted at the old and new Heath Steele Zn-Pb tailings impoundments, New Brunswick (Blowes 1990; Blowes et al. 1991). As H^+ is released by sulfide oxidation reactions, the tailings pore water becomes undersaturated with respect to calcite and dolomite, leading to calcite and dolomite dissolution buffering the pore-water pH between 6.5 and 7.5.

$$CaCO_3 + H^+ \rightleftharpoons Ca^{2+} + HCO_3^- \tag{6}$$

$$CaMg(CO_3)_2 + 2H^+ \rightleftharpoons Ca^{2+} + Mg^{2+} + 2HCO_3^- \tag{7}$$

Geochemical equilibrium calculations suggest that the precipitation of siderite, $Al(OH)_3$ and $Fe(OH)_3$ is favored as calcite and dolomite dissolve. Ferrous iron generated from sulfide oxidation can react with calcite to form siderite through:

$$CaCO_3 + Fe^{2+} \rightleftharpoons FeCO_3 + Ca^{2+} \tag{8}$$

or can react directly with HCO_3^- released from dissolution of calcite or dolomite to form secondary siderite (Morin and Cherry 1986, Ptacek and Blowes 1993). When calcite is completely consumed, the pore water pH abruptly declines, favoring dissolution of primary siderite originally present in gangue materials or secondary siderite. In the siderite-buffered zone the precipitation of $Al(OH)_3$ and $Fe(OH)_3$ is favored. As siderite dissolves, the pH is buffered to between pH 4.8 and pH 6.3. After siderite is completely consumed, the pH again declines abruptly until the dissolution of the next pH buffer in the series, $Al(OH)_3$, is favored. Dissolution of $Al(OH)_3$ buffers the pH to values

between approximately 4.0 to 4.3. When $Al(OH)_3$ is completely consumed, the pH declines, favoring the dissolution of $FeOH_3$ and resulting in pH values that fall below pH 3.5.

Sequences of similar pH-buffering zones have been observed at a number of tailings impoundments, including the Nordic Main U tailings impoundment (Dubrovsky et al. 1984a), the Waite Amulet Cu-Zn tailings impoundment (Blowes and Jambor 1990), the Copper Cliff Ni tailings impoundment (Coggans et al. 1994) and the Nickel Rim Ni tailings impoundment (Johnson 1993). At these sites, the amount of time required to deplete a given mineral phase and the relative thicknesses of the zones developed varied, depending on the original mass of solid-phase buffers contained in the gangue materials and on the initial mass of sulfide minerals. At other sites, where the H^+ generated by sulfide oxidation is less than the acid consumed by carbonate-mineral dissolution, such as at the Delnite site (Blowes 1990; Jambor and Blowes, 1991), the pore-water pH is controlled completely by carbonate-mineral dissolution, limiting the development of the remaining pH buffering zones.

The Effect of pH-Buffering Reactions on Trace Metal Mobility

Complete development of the pH-buffering sequence and its effect on the mobility of dissolved metals are illustrated by observations made at the Nickel Rim Ni tailings impoundment near Sudbury, Ontario (Johnson 1993). At the Nickel Rim site, sulfide oxidation in the vadose zone has released H^+ to the tailings water, resulting in low-pH ($2.1<pH<3.5$) conditions near the tailings surface. Interaction with H^+-consuming minerals has resulted in the progressive increase in pH with increasing depth observed in figure 2. Geochemical calculations conducted using MINTEQA2 (Allison et al. 1990) indicate that the pore waters approach or attain equilibrium with respect to $Fe(OH)_3$, $Al(OH)_3$, siderite and calcite, forming a series of pH-buffering zones moving downward from the tailings surface. The pH-buffering zones in figure 2 are labelled according to the dominant pH buffering process. Irregularities in the shapes of these pH-buffer zones are likely due to variations in the pore-water velocity, composition of the tailings solids and rates of acid generation.

At the Nickel Rim site, the pH of the tailings pore water has a strong effect on the movement of dissolved Al and Ni in the impoundment (fig. 2). At the interface between the Al-mineral pH-buffering zone and the siderite pH-buffering zone the concentration of dissolved Al decreases sharply. For example, at location NR2, located in the central portion of the tailings impoundment, the dissolved Al concentration decreases from > 1,150 mg/L to < 10 mg/L within a one meter interval (fig. 2). In this interval the pH increases from ~4 to ~5.8. Geochemical calculations conducted using MINTEQA2 indicate that the water samples from this location are saturated or slightly undersaturated with respect to amorphous $Al(OH)_3$ and supersaturated with respect to the crystalline aluminum hydroxide mineral gibbsite. These observations suggest that Al is removed from solution through the precipitation of an aluminum hydroxide or hydroxysulfate phase.

The concentration of dissolved Ni is also strongly dependent on the pore-water pH, showing a sharp decrease from > 250 mg/L to < 10 mg/L as the pH increases to above 5.8 within the siderite pH-buffering zone. Geochemical calculations conducted using MINTEQA2 suggest that the water at this depth is consistently undersaturated with respect to all of the secondary nickel-bearing hydroxide and hydroxysulfate phases included in the MINTEQA2 database. It is inferred therefore that Ni is removed from solution through adsorption or coprecipitation with the secondary ferric oxyhydroxide precipitates. Mineralogical study of the tailings solids indicated that the goethite contained near the surface of the tailings impoundment is Ni bearing (Jambor and Owens 1993), further suggesting that Ni is removed from the tailings pore water through adsorption or coprecipitation reactions.

Modelling Acid Neutralization and Trace-Metal Attenuation

The complexity of the interactions between the large number of dissolved constituents in the tailings pore waters and the large quantity of tailings solids make it difficult to determine *a priori* the changes in pH and metal ion mobility that are likely to occur as sulfide oxidation proceeds. Geochemical modelling of tailings pore water and mineralogical analysis of tailings solids can be used to delineate the principal reactions contributing to pH buffering

and metal attenuation (Dubrovsky 1986; Blowes 1990). Incorporation of the observed pH-buffering and metal-controlling reactions into a solute transport model allows calculations to be made to estimate the rate of dissolved metal migration. Using the multicomponent reactive solute transport model MINTRAN (Walter et al. 1994; Frind et al. 1994), simulations were conducted to estimate the migration of low-pH conditions through an underlying aquifer affected by acidic tailings water and their effect on the transport of dissolved metals. MINTRAN couples the geochemical speciation mass transfer model MINTEQA2 (Allison et al. 1990) with an efficient two-dimensional solute transport model (Frind et al. 1990). The model, as applied in this study, includes only equilibrium reactions and is limited, therefore, to conditions where the local equilibrium conditions apply.

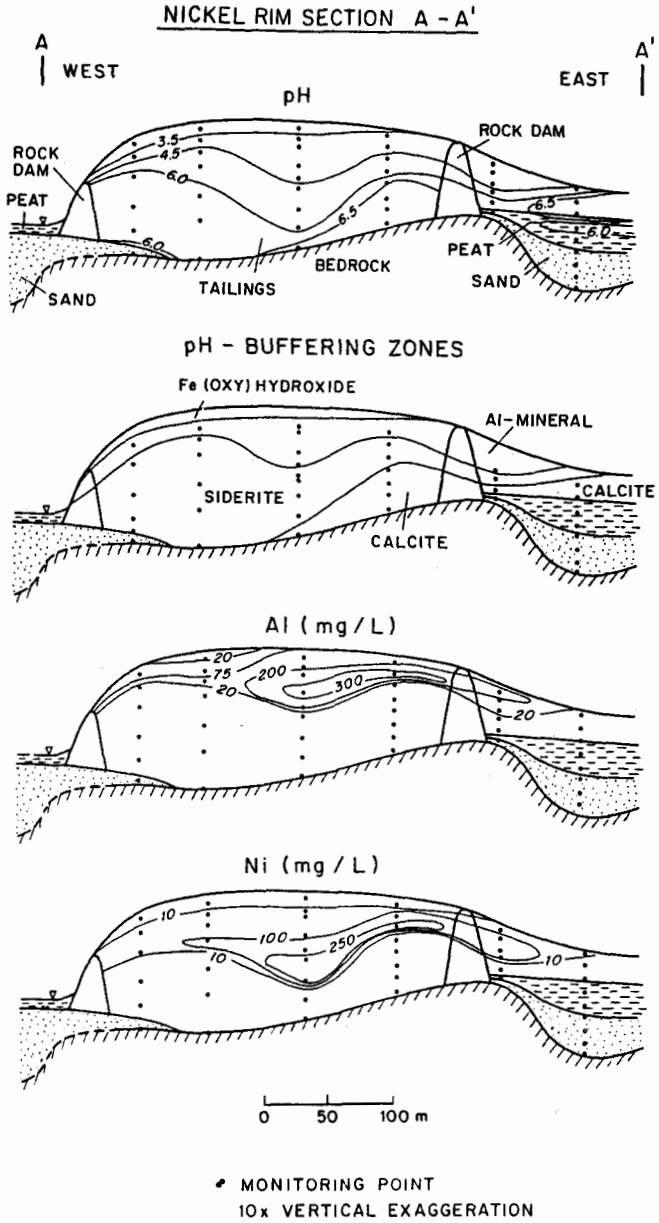

Figure 2. Values of pH, pH-buffering zones, and pore-water concentrations of Al and Ni in the Nickel Rim tailings impoundment near Sudbury, ON.

The simulations were based loosely on the description of the plume of tailings-derived water moving through an unconfined aquifer underlying the Nordic Main uranium tailings impoundment (Morin et al. 1988). The aquifer characteristics and tailings water compositions and background water compositions were selected to be similar to those at the field site. The aqueous components and initial mineral reserves included in the simulation are similar to those observed by Morin and Cherry (1988). The dissolved metals observed at the Nordic site include Al, Fe(II) and Fe(III). Important mineral phases include calcite, siderite, gibbsite, gypsum, amorphous silica and ferrihydrite. To enhance the generality of our simulation, we added higher concentrations of Pb, Cr and Mn and the associated mineral phases anglesite, cerussite, amorphous chromium hydroxide and rhodochrosite. This selection of phases was based on observations we have made at other field sites. In the model simulation, low-pH tailings water infiltrated into the source area of the aquifer for 24 years. The source area covers 10 m < x < 30 m at the watertable. The watertable boundary receives a flux of 0.142 m/yr., the downgradient boundary has a constant head of 13.6 m, and the left and lower boundaries are impermeable. The hydraulic conductivity is 2.5 x 10^{-6} m/s, the porosity is 0.3, the longitudinal dispersivity is 3.00 m, and the transverse dispersivity is 0.03 m.

The results of the simulations (figs. 3 and 4) show the development of a low-pH plume moving outward from the source area. Figure 3 shows contours and vertical profiles at x = 25 m for pH and dissolved Al, Cr and Pb and figure 4 shows solid-phase distributions for the associated mineral phases. The pH plume contains a series of pH plateaus similar to those observed in field studies (fig. 3). Far from the source, the pH ranges from 7.0 to 6.5 and is near equilibrium with respect to calcite, siderite and gibbsite. In this region of the aquifer, calcite is dissolving and siderite and gibbsite are accumulating. Closer to the source, the pH decreases sharply as the calcite initially

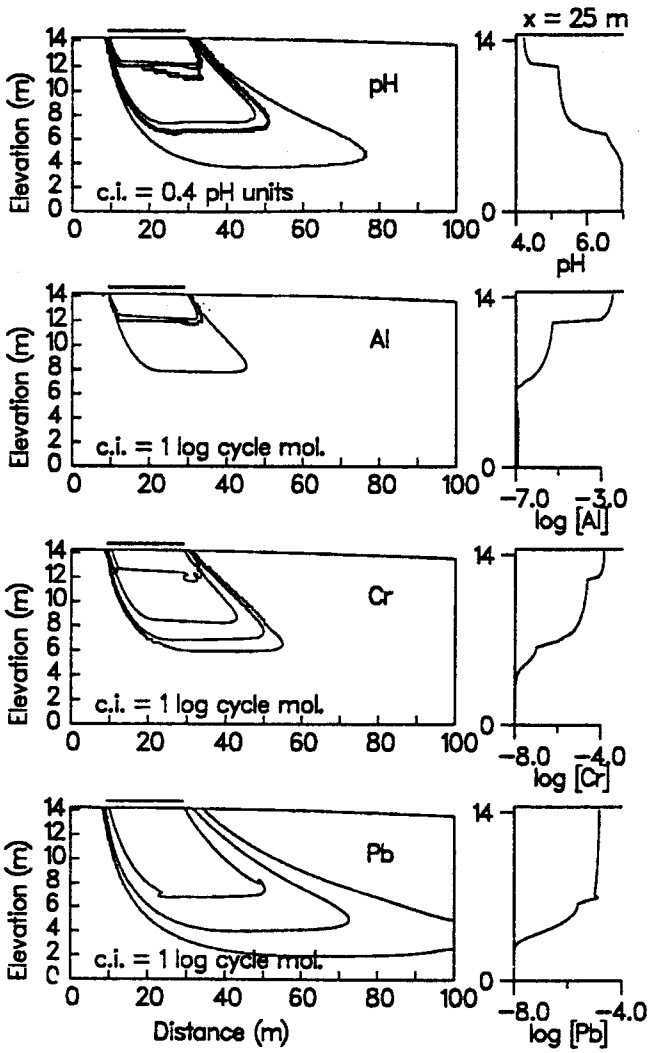

Figure 3. Simulated distributions of pH and concentrations of dissolved Al, Cr and Pb in aquifer receiving acidic drainage from a tailings impoundment at 24 years.

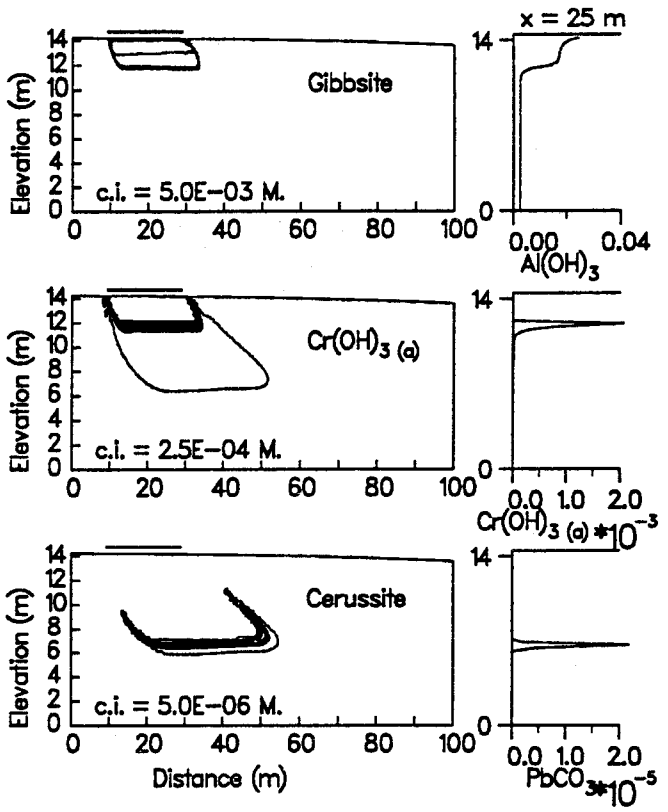

Figure 4. Simulated distributions of solid masses of gibbsite, amorphous $Cr(OH)_3$, and cerussite in aquifer receiving acidic drainage at 24 years.

present in the aquifer is depleted. At this front, the water becomes undersaturated with respect to calcite and the pH decreases from 6.5 to 5.5 (fig. 3) until equilibrium with respect to the second pH-buffering mineral siderite is attained. As siderite dissolves the mass of gibbsite continues to increase. Near the source, the pH decreases again as the primary and secondary siderite present in the aquifer is depleted. At this front, the pH decreases from 5.2 to 4.3 (fig. 3) and equilibrium with respect to gibbsite controls the pH from this point to the source. In this final region, the pH varies from 4.3 to 4.1.

The pH of the plume water affects the concentrations of the dissolved metals Al, Cr, and Pb assumed to be present in the plume. The secondary phases allowed to precipitate and dissolve include gibbsite, amorphous chromium hydroxide ($Cr(OH)_3$), and cerussite ($PbCO_3$). The mobilities of Al and Cr are dependent directly on the pH of the plume water, whereas the mobility of Pb is dependent on the activity of CO_3^{2-} , and therefore, indirectly dependent on the plume-water pH. The dissolved concentrations of Al and Cr show sharp decreases (fig. 3) that

correspond with the changes in pH accompanying the siderite and calcite dissolution fronts. These decreases are sufficient to lower the concentration of Cr to below the recommended concentration for drinking water (< 0.05 mg/L; OMOE 1983) and the Al concentration to below the recommended maximum concentration for the protection of freshwater aquatic life. The decreases in dissolved Cr and Al are accompanied by increases in the masses of gibbsite and $Cr(OH)_3$ retained in the aquifer (figs. 3 and 4). The total mass of $Cr(OH)_3$ is much less than the mass of gibbsite; the greatest accumulation of $Cr(OH)_3$ occurs at the siderite dissolution front. Lead is removed from the plume water through the precipitation of cerussite at the calcite dissolution front. Lead concentrations, however, remain above the recommended drinking water limit (< 0.01 mg/L, OMOE 1983) downstream of the cerussite precipitation front. Frind et al. (1994) conducted simulations describing the conditions in the aquifer following the period of sulfide oxidation, representing conditions where sulfide minerals have been depleted or an effective sulfide oxidation control put in place. These simulations show that the low solubilities of the metal-bearing precipitates are sufficient to maintain low concentrations of dissolved metals. The aqueous concentrations of all the metals considered, except Pb, decrease to below current regulatory guidelines shortly after the source of acidic drainage is terminated. These results suggest that metals precipitated in the aquifer are effectively immobilized under these conditions.

Summary and Conclusions

A series of acid-neutralization reactions controls the pore-water pH at four inactive mine tailings impoundments: the Waite Amulet Cu-Zn tailings impoundment (Blowes and Jambor 1990), the Heath Steele Pb-Zn tailings impoundment (Blowes et al. 1991), the Copper Cliff Ni tailings impoundment (Coggans et al. 1994) and the Nickel Rim Ni tailings impoundment (Johnson 1993). The sequence, calcite/dolomite dissolution, siderite dissolution, $Al(OH)_3$ dissolution, and $Fe(OH)_3$ dissolution, is the same as the pH-buffering sequence observed in the Nordic U tailings impoundment near Elliot Lake, Ontario (Dubrovsky 1986) and in a plume of tailings derived water adjacent to the Nordic tailings impoundment (Morin et al. 1988). The sequence of pH-buffering reactions observed at these inactive mine tailings impoundments results in the development of a series of pH regions that controls the mobility of several dissolved trace metals, including Al, Cr, Ni and Pb. The zones of pH buffering and metal attenuation are described well by a model which couples solute transport mechanisms with equilibrium geochemical reactions. Simulations conducted using this model suggest that in tailings impoundments with large masses of acid-consuming materials some of these metals may be retained in the tailings or underlying aquifers throughout the duration of acid release.

Literature Cited

Allison, J.D., D.S. Brown and K.J. Nova-Gradac. 1990. MINTEQA2/PRODEFA2, a geochemical assessment model for environmental systems: user's manual. Environmental Research Laboratory, Office of Research and Development, US EPA, Athens GA.

Bigham, J.M., U. Schwertmann, L. Carlson and E. Murad. 1990. A poorly crystallized oxyhydroxysulfate of iron formed by bacterial oxidation of Fe(II) in acid mine waters. Geochimica Cosmochimica Acta 54:2743-2758.

Blowes, D.W. 1990. The geochemistry, hydrogeology and mineralogy of decommissioned sulfide tailings: a comparative study. Ph.D. Thesis, University of Waterloo, Waterloo, ON, Canada, 637 pp.

Blowes, D.W. and J. L. Jambor. 1990. The pore-water geochemistry and the mineralogy of the vadose zone of sulfide tailings, Waite Amulet, Quebec, Canada. Applied Geochemistry 5:327-346.

Blowes, D.W., J.L. Jambor, E.J. Reardon and J.A. Cherry. 1994. The geochemical evolution of a high-sulfide mine tailings impoundment. Applied Geochemistry. In press.

Blowes, D.W., E.J. Reardon, J.L. Jambor and J.A. Cherry. 1991. The formation and potential importance of cemented layers in inactive sulfide mine tailings. Geochimica Cosmochimica Acta 55:965-978.

Cathles, L.M. 1979. Predictive capabilities of a finite difference model of copper leaching in low grade sulfide waste dumps. Mathematical Geology 11: 175-191.

Coggans, C.J., D.W. Blowes, W.D. Robertson and J.L. Jambor. 1994. The hydrogeochemical evolution of a nickel mine tailings impoundment, Copper Cliff, Ontario. Reviews in Economic Geology, In press.

Davis, G.B. and A.I.M. Ritchie. 1986. A model of oxidation in pyritic mine wastes. I. Equations and approximate solution. Applied Mathematical Modelling 10: 314-322.

Dubrovsky, N.M. 1986. Geochemical evolution of inactive pyritic tailings in the Elliot Lake uranium district, Ph.D. Thesis, University of Waterloo, Waterloo, ON, Canada.

Dubrovsky, N.M., J.A. Cherry, E.J. Reardon and A.J. Vivyurka. 1984a. Geochemical evolution of inactive pyritic tailings in the Elliot Lake Uranium district: 1. The groundwater zone. Canadian Geotechnical Journal 22:110-128.

Dubrovsky, N.M., K.A. Morin, J.A. Cherry, D.J.A. Smyth. 1984b. Uranium tailings acidification and subsurface contaminant migration in a sand aquifer. Water Pollution Research Journal of Canada 19:55-89.

Ferguson, K.D. and P.M. Erickson. 1987. Will it generate AMD? An overview of methods to predict acid mine drainage. p. 215-244. In Proceedings Acid Mine Drainage Seminar/Workshop (Halifax, Nova Scotia, March 23-26, 1987).

Frind, E.O., D.W. Blowes, J.W. Molson and C.J. Ptacek. 1994. Simulation of multicomponent reactive transport in groundwater. Submitted to the International Symposium on Transport and Reactive Processes in Aquifers, ETH, Zurich, Switzerland, April 11-15, 1994.

Frind, E.O., W.H.M. Duynisveld, O. Strebel and J. Boettcher. 1990. Modeling of multicomponent transport with microbial transformation in groundwater: The Fuhrberg case. Water Resources Research 26:1707-1719.

Jambor, J.L. 1987. Mineralogical and chemical investigation of cores from piezometric sites in Waite Amulet tailings, Noranda, Quebec. Division Report MSL 87-32(IR), CANMET, Energy, Mines and Resources, Canada.

Jambor, J.L. and D.W. Blowes. 1991. Mineralogical study of low-sulphide, high-carbonate, arsenic-bearing tailings from the Delnite minesite, Timmins, Ontario. In Proceedings of the Second International Conference on the Abatement of Acidic Drainage. (Montreal, Quebec, September 16-18, 1991).

Jambor, J.L. and D.R. Owens. 1993. Mineralogy of the tailings impoundment at the former Cu-Ni deposit of Nickel Rim Mine Ltd., eastern edge of the Sudbury structure, Ontario. Division Report MSL 93-4 (CF), CANMET, Energy, Mines and Resources, Canada, 92 p.

Johnson, R.H. 1993. The physical and chemical hydrogeology of the Nickel Rim Mine tailings, Sudbury, Ontario. M.Sc. Thesis, University of Waterloo, Waterloo, Ontario, Canada, 108 p.

Morin, K.A. 1983. Prediction of subsurface contaminant transport in acidic seepage from uranium tailings impoundments. Ph.D. Thesis, University of Waterloo, Waterloo, Ontario, Canada.

Morin, K.A. and J.A. Cherry. 1986. Trace amounts of siderite near a tailings impoundment, Elliot Lake, Ontario, and its implication in controlling contaminant migration in a sand aquifer. Chemical Geology 56:117-134.

Morin, K.A. and J.A. Cherry. 1988. Migration of acidic groundwater seepage from uranium-tailings impoundments. 3. Simulation of the conceptual model with application to seepage area A. Journal of Contaminant Hydrology 2:323-342.

Morin, K.A., J.A. Cherry, N.K. Dave, T.P. Lim, A.J. Vivyurka. 1988. Migration of acidic groundwater seepage from uranium-tailings impoundments. 1. Field study and conceptual hydrogeochemical model. Journal of Contaminant Hydrology 2:271-303.

Nicholson, R.N., R.W. Gillham amd E.J. Reardon. 1990. Pyrite oxidation in carbonate-buffered solution. 2. Rate control by oxide coatings. Geochimica Cosmochima Acta 54: 395-402.

Ontario Ministry of the Environment (OMOE) 1983. Ontario drinking water objectives. Ontario Ministry of the Environment, Toronto, Ontario, Technical Report, 56 pp.

Ptacek, C.J. and Blowes, D.W. 1993. Influence of siderite on the geochemistry of inactive mine tailings impoundment. p. 172-189. In Environmental Geochemistry of Sulfide Oxidation, C.N. Alpers and D.W. Blowes (Eds.), American Chemical Society Symposium Series, Vol. 550.

Smyth, D.J.A. 1981. Hydrogeological and geochemical studies above the water table in an inactive uranium tailings impoundment near Elliot Lake, Ontario. M.Sc. Project, University of Waterloo, Waterloo, Ontario.

Walter, A.L., E.O. Frind, D.W. Blowes, C.J. Ptacek and J.W. Molson. 1994. Modelling of multicomponent reactive transport in aquifers impacted by mine tailings effluents. Water Resources Research, in press.